The Survival Pathways Phosphatidylinositol-3 Kinase (PI3-K)/Phosphoinositide-Dependent Protein Kinase 1 (PDK1)/Akt Modulate Liver Regeneration Through Hepatocyte Size Rather Than Proliferation

Sanae Haga,[1,2] Michitaka Ozaki,[3] Hiroshi Inoue,[4] Yasuo Okamoto,[5] Wataru Ogawa,[5] Kiyoshi Takeda,[6] Shizuo Akira,[7] and Satoru Todo[1]

Liver regeneration comprises a series of complicated processes. The current study was designed to investigate the roles of phosphoinositide-dependent protein kinase 1 (PDK1)-associated pathways in liver regeneration after partial hepatectomy (PH) using liver-specific *Pdk1*-knockout (L-*Pdk1*KO) and *Pdk1/STAT3* double KO (L-DKO) mice. There was no liver regeneration, and 70% PH was lethal in L-*Pdk1*KO mice. Liver regeneration was severely impaired equally in L-*Pdk1*KO and L-DKO mice, even after nonlethal 30% PH. There was no cell growth (measured as increase of cell size) after hepatectomy in L-*Pdk1*KO mice, although the post-PH mitotic response was the same as in controls. As expected, hepatectomy did not induce hepatic Akt-phosphorylation (Thr308) in L-*Pdk1*KO mice, and post-PH phosphorylation of Akt, mammalian target of rapamycin (mTOR), p70 ribosomal S6 kinase ($p70^{S6K}$), and S6 were also reduced. To examine the specific role of PDK1-associated signals, a "pif-pocket" mutant of PDK1, which allows PDK1 only to phosphorylate Akt, was used. Liver regeneration was recovered in L-*Pdk1*KO mice with a "pif-pocket" mutant of PDK1. This re-activated Akt in L-*Pdk1*KO mice liver and induced post-PH cell growth, without affecting cell proliferation. Further deletion of STAT3 (L-DKO mice) did not further deteriorate liver regeneration, although this certainly reduced post-PH mitotic response. These findings indicate that PDK1/Akt contribute to liver regeneration by regulating cell size. Regarding phosphatidylinositol-3 kinase (PI3-K), immediate upstream signal of PDK1, activation of PI3-K induced cell proliferation via STAT3 activation in the liver of L-*Pdk1*KO mice but did not improve impaired liver regeneration. This confirmed the pivotal role of PDK1 in liver regeneration and cell growth. *Conclusion:* PDK1/Akt-mediated responsive cell growth is essential for normal liver regeneration after PH, especially when cell proliferation is impaired. (HEPATOLOGY 2009;49:204-214.)

Abbreviations: BrdU, bromodeoxyuridine; L-DKO, liver-specific Pdk1/Stat3 double knockout; L-Pdk1KO, liver-specific Pdk1 knockout; L-Stat3KO, liver-specific Stat3 knockout; mTOR, mammalian target of rapamycin; myr-p110, myristoylated form of p110 (catalytic subunit) of PI3-K; PCNA, proliferating cell nuclear antigen; PDK1, phosphoinositide-dependent protein kinase 1; PH, partial hepatectomy; pif, PDK1-interacting fragment; PI3-K, phosphatidylinositol-3 kinase; $p70^{S6K}$, p70 ribosomal S6 kinase; SEM, standard error of the mean; STAT3, signal transducer and activator of transcription protein 3; S6, ribosomal S6; WB, western blot

From the [1]Department of Surgery, Hokkaido University School of Medicine, Sapporo, Japan; [2]Research Fellow of the Japanese Society for the Promotion of Science (JSPS), Tokyo, Japan; the [3]Department of Molecular Surgery, Hokkaido University School of Medicine, Sapporo, Japan; [4]Frontier Science Organization, Kanazawa University, Ishikawa, Japan; the [5]Division of Diabetes and Digestive and Kidney Diseases, Department of Clinical Molecular Medicine, Kobe University Graduate School of Medicine, Kobe, Japan; the [6]Laboratory of Immune Regulation, Department of Microbiology and Immunology, Graduate School of Medicine Osaka University, Osaka, Japan; and the [7]Laboratory of Host Defense, WPI Immunology Frontier Research Center, Osaka University, Osaka, Japan.

Received April 16, 2008; accepted August 11, 2008.

Supported by a Grant-in-Aid for Scientific Research from the Ministry of Education, Culture, Sports, Science, and Technology of Japan (#17390357 and #19659317 to M.O.).

Address reprint requests to: Michitaka Ozaki MD, PhD, Department of Molecular Surgery, Hokkaido University School of Medicine, N-15, W-7, Kita-ku, Sapporo, Hokkaido, 060-8638 Japan. E-mail: mozaki@m07.itscom.net; ozaki-m@med.hokudai.ac.jp; fax: (81)-11-717-7515.

Published online in Wiley InterScience (www.interscience.wiley.com).

DOI 10.1002/hep.22583

Potential conflict of interest: Nothing to report.

Additional Supporting Information may be found in the online version of this article.

Liver regeneration is a physiopathological phenomenon of quantitative recovery from loss of liver mass to compensate for decreased hepatic volume and impaired function. The liver has a unique ability to restore lost volume, rarely seen in other organs.[1,2] It is well established that normal adult hepatocytes are usually quiescent but have the potential ability to replicate. After surgical procedures that reduce liver mass, such as partial hepatectomy (PH) or live donor liver transplantation, rapid enlargement of the residual or grafted liver commonly takes place to restore liver mass and function. Clinically, liver regeneration has important implications because many therapeutic strategies for surgical treatment of liver diseases such as removal of liver tumors and liver transplantation depend on the ability of liver to regenerate physically and functionally. Poor or insufficient liver regeneration may be potentially fatal for these patients.[3-5] Therefore, better understanding of the physiopathological features of liver regeneration could lead to clinical benefits.

Numerous studies so far have sought to elucidate the mechanisms responsible for liver regeneration, investigating the regulation of cell proliferation in simple rodent hepatectomy models.[6-11] The importance of interleukin-6/signal transducer and activator of transcription-3 (STAT3) pathway in liver regeneration has been established, as reported by a number of researchers[12,13] using liver-specific *Interleukin-6* or *Stat3* knockout mice. Regarding STAT3, it was found that the defective mitotic response to hepatectomy in liver-specific *Stat3*-KO (L-*Stat3*KO) mice did not affect physical and functional liver regeneration at all.[6] Although the hepatocyte mitotic response was suppressed or greatly delayed in L-*Stat3*KO mice, Akt and its associated signaling molecules such as p70 ribosomal S6 kinase ($p70^{S6K}$), mammalian target of rapamycin (mTOR), and glycogen synthase kinase-3 were immediately phosphorylated after PH. These findings suggest that when cell proliferation is impaired, these molecules mediate a possible compensatory mechanism of liver regeneration.

The phosphatidylinositol-3 kinase (PI3-K)/phosphoinositide-dependent protein kinase 1 (PDK1)/Akt pathway, known as a survival pathway, targets various molecules involved in anti-apoptosis, anti-oxidation, and protein synthesis.[14-18] Recent reports have shown that PI3-K/PDK1/Akt pathway and its associated molecules are responsible for determining cell size and functions.[6,19-24] Many of these studies used animals with targeted gene disruption to demonstrate the crucial roles of these molecules (mTOR, $p70^{S6K}$, and glycogen synthase kinase-3) in determining the "inherent size of cells" in the specific organ. In contrast, liver-specific knockout of *phosphatase tensin homolog deleted on chromosome 10,* a negative regulator of PI3-K/Akt pathway, induced enlargement of the organ. Persistent stimulation of PI3-K/Akt pathway in hepatocytes resulted in an enlarged liver mass mainly by stimulating glycogen/fatty acid synthesis.[25] Because the PI3-K/Akt pathway is certainly involved in glucose/fat metabolism as well as protein metabolism in the liver,[26,27] these findings suggest a crucial role for these molecules in cell growth and liver regeneration during an acute response, such as occurs post-PH. However, the role of this pathway in acute responses to such stimuli has not yet been clearly determined.

We hypothesized that PI3-K/PDK1 plays a pivotal role in liver regeneration by positively regulating cell growth, especially in cases in which cell proliferation is severely impaired. The current study was therefore designed to further examine the roles of PI3-K/PDK1 and associated molecules in liver regeneration and to determine the molecule(s) critically responsible for post-PH liver regeneration in mice.

Materials and Methods

Generation of Liver-Specific Knockout Mice. We generated liver-specific *Pdk1*-knockout (L-*Pdk1*KO) mice and liver-specific *Pdk1/Stat3* double knockout (L-DKO) mice,[28] which harbor a transgene for Cre-recombinase under the control of albumin gene promoter and are homozygous for a floxed allele of *Pdk1* or both *Pdk1* and *Stat3*, respectively, by crossing Alb-*Cre* mice[29] with *Pdk1*-flox mice and *Stat3*-flox; *Pdk1*-flox mice, respectively. We used *Stat3*-flox/flox and *Pdk1*-flox/flox littermates as controls for L-*Pdk1*KO and L-DKO mice, respectively. Although mice with a liver-specific deficiency of PDK1 were previously shown to develop a severe condition characterized by prominent edema and premature death,[27] L-*Pdk1*KO mice generated in the current study appeared normal until at least 6 months of age. The metabolic phenotypes of L-*Pdk1*KO and L-DKO mice have been described elsewhere.[28]

Animal Experiments. L-*Pdk1*KO, L-DKO, and C57BL/6 mice (male, 8-10 weeks) were used for simple 70%/30% PH experiments. Anesthesia was induced with an intraperitoneal injection of Nembutal (pentobarbital sodium, 60 mg/100 g body weight). Mice were fasted overnight before the experiments. After laparotomy, the left and median liver lobes were surgically resected for 70% PH, and the left lobe for 30% PH. The mice were sacrificed for collection of liver specimens at the indicated times before or after hepatectomy, and the liver/body weight ratios were calculated to estimate the recovery of liver mass. The animals were maintained under standard

conditions and treated according to the Guidelines for the Care and Use of Laboratory Animals of Hokkaido University School of Medicine.

Cell Proliferation Assay. To evaluate proliferation of hepatocytes after PH, proliferating cell nuclear antigen (PCNA)-positive, bromodeoxyuridine (BrdU)-labeled hepatocytes and mitotic hepatocytes were counted. Liver tissues were removed before and 48 hours or 72 hours after hepatectomy (for PCNA and BrdU or mitosis assessment, respectively), fixed in 10% buffered formalin, and paraffin embedded. Hematoxylin-eosin staining and immunohistochemical staining with anti-PCNA were performed. For BrdU labeling assay, BrdU labeling reagent was injected intravenously into mice at 1 mL/100 g body weight 1 hour before sacrifice. BrdU was immunostained with anti-BrdU antibody according the manufacturer's recommendations (Roche, Basel, Switzerland). At least 500 hepatocytes were counted for mitotic or PCNA/BrdU positivity at least three times in different sections in each group.

Electrophoretic Mobility Shift Assay. STAT3 DNA-binding activity was assayed using mutant 67 of serum inducible element of c-fos gene promoter (SIE-m67) oligonucleotide as a probe (5′-actgGGATTTTTC-CCGTAAATGGTC-3′). The reaction mixture contained nuclear protein extract (5 μg), dithiothreitol (2 mM), poly(deoxyinosinic-deoxycytidylic) acid sodium salt (dI-dC) (2 μg), single-stranded DNA (10 μg/mL), and ^{32}P-labeled SIE-m67 probe (5×10^5 cpm). The specimens were electrophoresed on 5% polyacrylamide native gels at 4°C in 0.25× Tris-Borate/ethylenediaminetetra-acetic acid buffer.

Western Blot Analysis. Thirty micrograms whole liver protein extract was separated by 10% sodiumk dodecyl sulfate polyacrylamide gel electrophoresis and transferred to a nitrocellulose membrane. The following antibodies were used as primary antibodies: PDK1, STAT3/phospho-STAT3 (Santa Cruz, CA), Akt/phospho-Akt (Thr and Ser), p70^{S6K}/phospho-p70^{S6K}, mTOR/phospho-mTOR (Cell Signaling, MA), and PCNA (Santa Cruz, CA).

Measurement of Cell Size. The method to measure the size of hepatocytes in liver sections was described previously.[6] Briefly, individual hepatocytes were outlined and cross-sectional area was determined with a computer-assisted image analysing system (LSM Image Browser, Carl Zeiss GmBH, Jena, Germany). Cell areas of at least 500 hepatocytes were randomly selected in zone 2 and calculated in triplicate using different sections in each group.

Adenoviral Vectors (LacZ, L155E, and myr-p110). The replication-deficient adenovirus encoding *β-galactosidase* was used as a control vector (LacZ). An adenovirus vector encoding PDK1-interacting fragment (pif)-pocket mutant of *Pdk1*(L155E) was generated, where Leu155 was replaced by Glu, allowing PDK1 signaling exclusively to Akt, but not to p70^{S6K} or any others.[30] An adenovirus vector encoding a hemagglutinin-tagged myristoylated form of p110 (catalytic subunit) of PI3-K (myr-p110) was generated as described previously.[31] All viruses were produced in human embryonic kidney 293 cells, purified on double cesium chloride gradients, and plaque-titered. All adenoviruses were injected intravenously via tail vein 72 hours before the experiments.

Statistical Analysis. Results are expressed as means ± standard error of the mean (SEM). Statistical analyses were performed with Fishers' test, and P values less than 0.05 were considered significant.

Results

L-Pdk1KO Mice and L-DKO Mice. Western blot (WB) analyses showed the expression of PDK1 and PDK1/STAT3 in the livers of L-*Pdk1*KO and L-DKO mice, respectively (Fig. 1A). Only a trace amount of PDK1 was detected in L-*Pdk1* KO liver, but no PDK1 and STAT3 were detected in L-DKO liver. These mice, however, showed normal liver structure and morphology (Fig. 1B), as reported previously.[27] Liver and body weights of these knockout mice were no different from control mice at 8 to 10 weeks of age (data not shown).

Survival and Liver Regeneration After Hepatectomy in L-Pdk1KO Mice and L-DKO Mice. Six of 10 L-*Pdk1*KO mice with conventional 70% PH died within 12 hours. Liver regeneration of the remaining four L-*Pdk1*KO mice was severely impaired (Fig. 2A). However, 30% PH allowed all mice to survive until at least 14 days post-PH (Fig. 2B). Liver/body weight ratios showed that estimated liver regeneration was significantly and persistently suppressed at this time in L-*Pdk1*KO mice. Because albumin is produced exclusively by hepatocytes, serum levels of albumin were measured to evaluate functional liver regeneration after PH in L-*Pdk1*KO mice (Fig. 2C). It was found that serum albumin levels were maintained in the normal range even after PH in control mice, but were still reduced 2 weeks post-PH in L-*Pdk1*KO mice. These data thus suggest that PDK1 is essential for the recovery of liver mass and function after hepatectomy. Regarding the other markers of liver function/injury, serum levels of glutamic oxaloacetic transaminase/glutamate pyruvate transaminase/lactate dehydrogenase and bilirubin did not differ between control and L-*Pdk1*KO mice before PH, and were moderately increased after PH, showing somewhat higher levels in the latter mice (Fig. 2D). Blood glucose levels were decreased

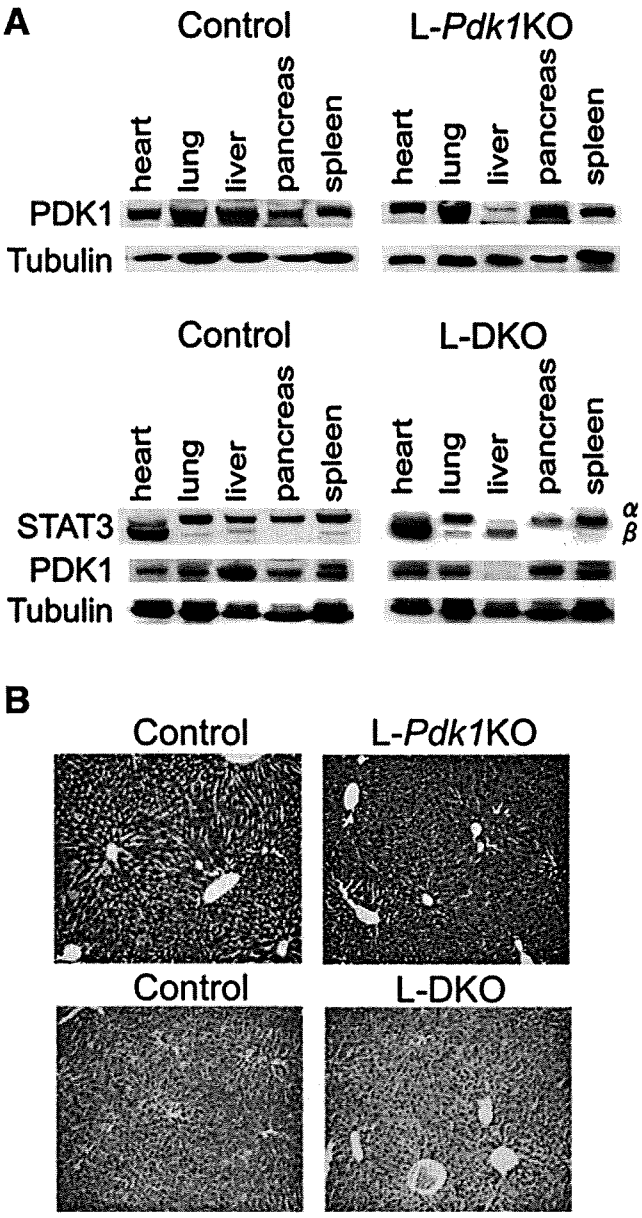

Fig. 1. Expression of PDK1 and STAT3 in liver tissues (A) and liver histology (B) in L-*Pdk1*KO and L-DKO mice. (A) WB showing liver-specific deletion of PDK1 and PDK1/STAT3 in L-*Pdk1*KO and L-DKO mice, respectively. (B) Hematoxylin-eosin staining showing normal liver structure of both L-*Pdk1*KO and L-DKO mice (original magnification ×200)

after PH but did not show any difference between the two groups.

Apoptotic cell death was very mildly induced by PH equally in control and L-*Pdk1* KO liver, but did not differ between the groups (Fig. 2E). This fact indicates that apoptotic cell death did not contribute to the reduced liver mass recovery in L-*Pdk1* KO mice.

Mitotic Responses in L-Pdk1KO Mice After Hepatectomy. Mitotic responses began immediately after PH in L-*Pdk1*KO mice even though liver regeneration was severely impaired (Fig. 3). Mitotic hepatocytes 3 days post-PH (Fig. 3A) and BrdU/PCNA-positive hepatocytes 2 days post-PH (Fig. 3B and C) were equally apparent in control and L-*Pdk1*KO mice. The numbers of mitotic cells, BrdU-positive cells, and PCNA-positive cells observed at each time (48 hours, 72 hours) in the post-PH liver tissues were not statistically different between the groups. BrdU incorporation into nuclei, as well as PCNA expression, also remained identical. These data suggest that deletion of PDK1 in liver did not affect the initial mitotic response of hepatocytes after PH.

In support of these observations, STAT3, which is a pivotal transcription factor in the post-PH mitotic response, showed similar activity in both control and L-*Pdk1*KO mice (Fig. 3D). Phosphorylation of STAT3 at Tyr705 and Ser727 and its binding to DNA occurred immediately after PH, and recovered to basal levels by 72 hours in both knockout and control mice. STAT3 activation after PH also did not differ in its intensity and timing in control and L-*Pdk1*KO mice.

Cell Size (Cell Growth) After Hepatectomy and Activation of PDK1-Associated Signals. Hepatocyte cell size in L-*Pdk1*KO mice without PH was slightly smaller than in controls, but the difference was not statistically significant (Fig. 4A). Cell size in normal livers increased significantly after PH, but not in L-*Pdk1*KO mice; rather, there was a tendency to decrease in the latter.

PDK1 specifically phosphorylates Akt at Thr308, and its activity can be assessed in this way (Fig. 4B). We found that Akt was phosphorylated at Thr308 immediately but transiently after PH in controls, but not in L-*Pdk1*KO livers up to 14 days post-PH. Akt phosphorylation at Thr308 was completely abolished in L-Pdk1 KO liver. This means that the liver of L-*Pdk1* KO mice is enough to study the function of PDK1, although PDK1 expression is slightly detected in L-*Pdk1* KO liver (Fig. 1A). Interestingly, Akt was strongly and persistently phosphorylated at Ser473 in L-*Pdk1*KO liver even in the quiescent state, as well as after PH, although this is normally carried out by PI3-K–regulated kinases other than PDK1. Also, the increased amounts of total Akt were observed in L-*Pdk1* KO liver, which may be the result of increased production of Akt in response to the reduced signal from PDK1.

Among the molecules downstream of PDK1, Akt, mTOR, $p70^{S6K}$, and S6 may potentially contribute to the maintenance of normal liver regeneration when cell proliferation is suppressed.[6] To confirm the involvement of these molecules in the impairment of liver regeneration in L-*Pdk1*KO mice, phosphorylation (activation) of mTOR, $p70^{S6K}$, and S6, downstream targets of $p70^{S6K}$, as well as Akt, was also examined (Fig. 4B). Mtor and $p70^{S6K}$ were weakly phosphorylated even in quiescent liver. Al-

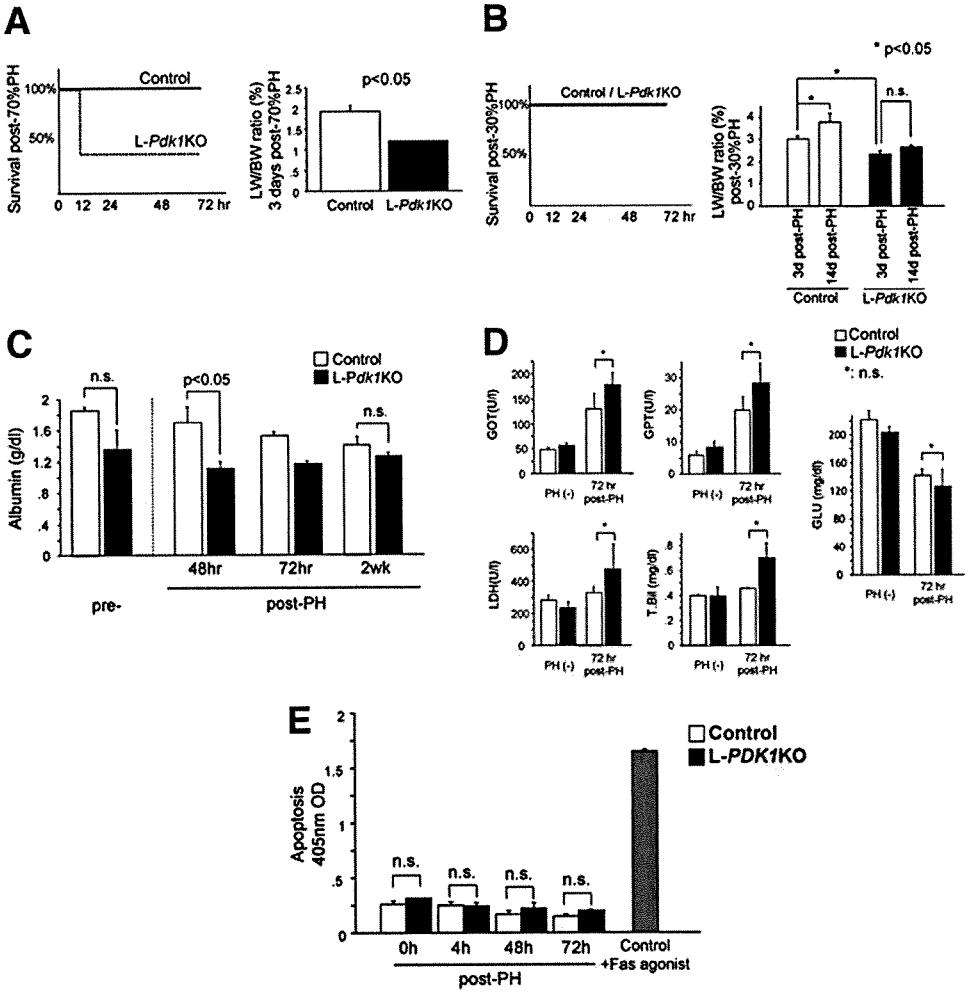

Fig. 2. Impaired liver regeneration after PH in L-*Pdk1*KO mice. (A) Seventy percent PH was lethal within 12 hours with no liver regeneration. (B) Thirty percent PH allowed the L-*Pdk1*KO mice to survive at least until 14 days post-PH with no liver regeneration. (C) Serum albumin levels were reduced in L-*Pdk1*KO mice transiently after PH. (D) Serum levels of glutamic oxaloacetic transaminase/glutamate pyruvate transaminase/lactate dehydrogenase and bilirubin and blood glucose level were measured pre-PH and post-PH. No significant differences were observed between control and L-*Pdk1*KO mice. Data are from at least three independent experiments, expressed as mean ± SEM.

though mTOR, $p70^{S6K}$, and S6 were all phosphorylated markedly from 4 hours after PH up until 72 hours in controls, they were not or were only very weakly phosphorylated in L-*Pdk1*KO liver after PH. S6 was markedly phosphorylated even at quiescence, which was slightly and transiently increased after PH in control livers. Deletion of PDK1 suppressed post-PH phosphorylation of S6, which quickly returned to the pre-PH level up to 72 hours post-PH in L-*Pdk1*KO liver regardless of liver mass recovery. $p70^{S6K}$ responded immediately to PH and possibly phosphorylated S6, but the latter is presumably also phosphorylated by kinases other than $p70^{S6K}$. Taken together, these findings may suggest the possibility that PDK1-Akt(/mTOR) pathway plays a more important role in post-PH liver regeneration by cell growth, even though $p70^{S6K}$/S6 pathway is certainly involved in cell growth in other types of cells.[32,33]

PDK1/Akt-Mediated Liver Regeneration by Cell Growth Rather than Cell Proliferation. To confirm the role of PDK1-Akt/mTOR pathway in liver regeneration, we employed the "pif-pocket" mutant of PDK1, which allows PDK1 to signal exclusively to Akt but not to $p70^{S6K}$ or others.[30,34-36] Adenovirus-mediated introduction of the pif-pocket mutant (L155E) did re-phosphorylate Akt (Thr308), but not $p70^{S6K}$ (Thr389), 4 hours after PH in L-*Pdk1*KO mice (Fig. 5A). Re-activation of Akt, but not $p70^{S6K}$, in L-*Pdk1*KO mice allowed responsive cell growth again in the post-PH liver without affecting cell proliferation, and eventually improved liver regeneration in L-*Pdk1*KO mice (Fig. 5A, B).

We also performed the experiment of 70% PH with hepatic introduction of the pif-pocket mutant (L155E), to confirm the effect of Akt on liver cell growth or proliferation after PH (Fig. 5C). Hepatic introduction of pif-pocket mutant let the 70% PH mice survive at least until 72 hours post-PH and recovered liver sufficiently. Post-PH mitosis and cell growth in L-*Pdk1* KO liver were observed to the same degree as the post-PH liver of control mice.

Furthermore, we performed an additional experiment to ask whether $p70^{S6K}$ indeed has no influence on hepatocyte cell size. Sodium salicylate, a known inhibitor of $p70^{S6K}$,[37,38] clearly suppressed phorbol myristate acetate–

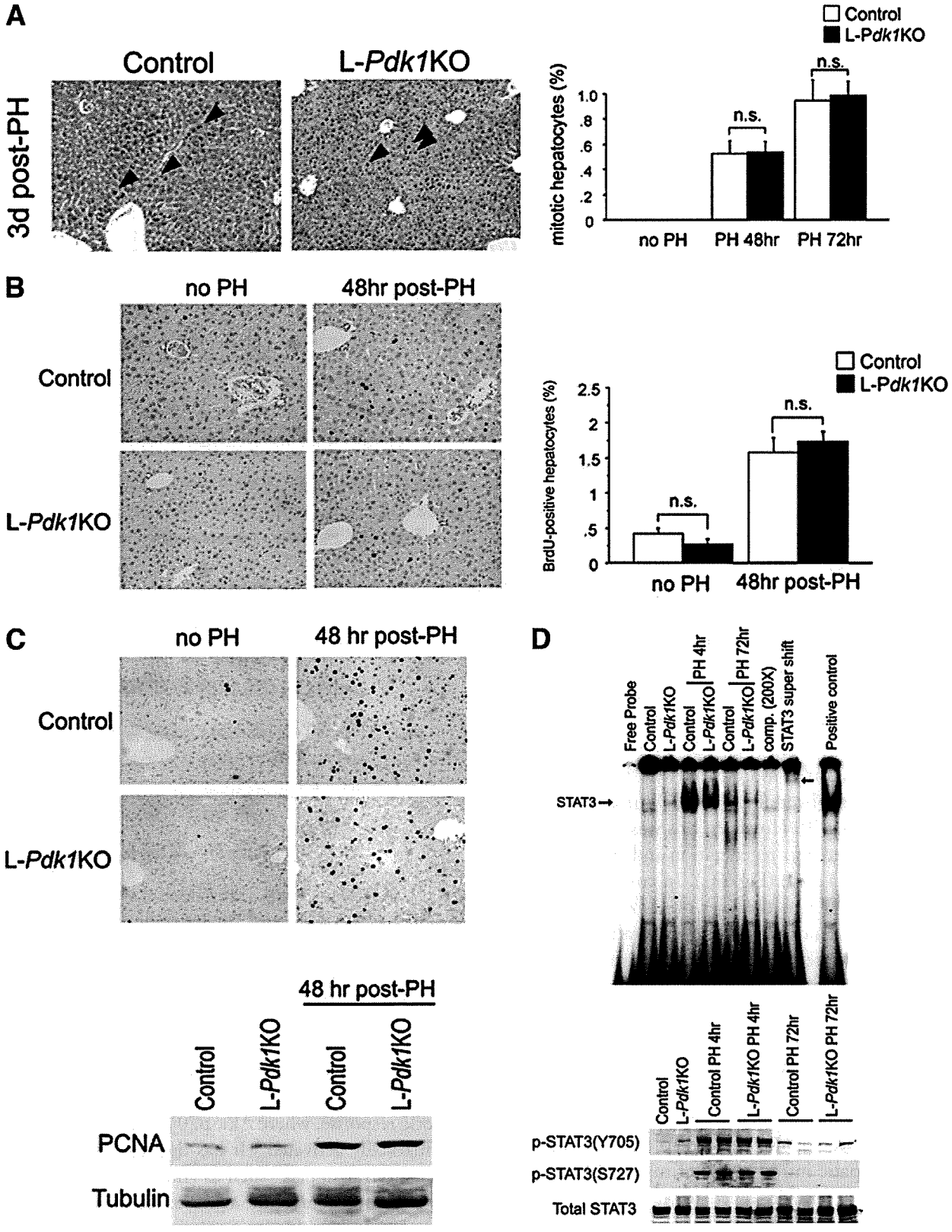

Fig. 3. Normal mitotic response after PH in L-*Pdk1*KO mice. (A) Hematoxylin-eosin staining showing mitotic hepatocytes 48 and 72 hours post-PH in control and L-*Pdk1*KO liver. (Arrowheads indicate mitotic hepatocytes. Original magnification ×200) Counts of mitotic, BrdU-positive, and PCNA-positive hepatocytes (immunohistochemistry and WB) in the regenerating liver document equivalent mitotic responses in control and L-*Pdk1*KO liver (A, B, C). Each photo is representative of at least three independent experiments. Data are expressed as mean ± SEM. (D) WB and electrophoretic mobility shift assays showing STAT3 phosphorylated (Tyr705 and Ser727) and activated to the same extent in control and L-*Pdk1*KO liver. Each blot is representative of at least three independent experiments.

induced phosphorylation of p70^{S6K} in hepatocytes (Fig. 5D) but had no effect on Akt (data not shown). Inhibition of p70^{S6K} did not affect hepatocyte cell size but slightly suppressed cell proliferation (Fig. 5D). This may suggest that p70^{S6K} is involved mainly in transmitting mitotic signals, not cell growth signals. These data are consistent with our hypothesis that the PDK1–Akt pathway, but not PDK1–p70^{S6K}, plays a pivotal role in liver regeneration mainly by regulating cell size.

Activation of PI3-K Does Not Improve Post-PH Liver Regeneration in L-Pdk1KO Mice. To confirm the pivotal role of PDK1 in liver regeneration, we performed additional experiments to investigate the effects of PI3-K, a signaling molecule immediately upstream of PDK1, on liver regeneration in L-*Pdk1*KO mice.

In controls, activation of PI3-K by transducing myr-p110 leads to phosphorylation of Akt (Thr308 and Ser473) and STAT3 (Tyr705) in a dose-dependent manner and results in enlarged livers without PH (Fig. 6A). This may indicate that PI3-K signals to STAT3 for cell proliferation as well as Akt for cell growth, and contributes cooperatively to liver regeneration. An adenovirus vector of myr-p110 was injected to L-*Pdk1*KO mice at the time of PH (1×10^8 pfu/body). It was found that myr-p110 phosphorylated Akt at Thr308 and Ser473 in control mice, but only at Ser473 in L-*Pdk1*KO mice, because Akt Thr308 is phosphorylated only by PDK1 whereas Ser473 can be phosphorylated by PI3-K–regulated kinases other than PDK1 (Fig. 6B). Hepatic activation of PI3-K clearly induced more PCNA-positive and mitotic hepatocytes in the liver of L-*Pdk1*KO mice after PH than in controls (Fig. 6B). However, this was not sufficient to improve impaired liver regeneration and albumin synthesis in L-*Pdk1*KO mice (Fig. 6C). In contrast, additional deletion of STAT3 in the liver of L-*Pdk1*KO mice (L-DKO mice) did not affect its regeneration (Fig. 6D). These data indicate that PI3-K is important for the increase of liver mass by signaling STAT3 for cell proliferation and PDK1/Akt for cell growth, but cannot mediate liver regeneration if PDK1/Akt pathway is disturbed. PDK1-mediated signals for cell growth are thus crucial for liver regeneration.

To confirm the contribution of PI3-K/STAT3 to post-PH cell growth, we performed 30% PH in DKO mice with hepatic introduction of myr-p110. Constitutive activation of PI3-K failed to increase post-PH cell proliferation and growth, or to improve the impaired liver regeneration in DKO mice (Fig. 6E).

Discussion

Important roles for interleukin-6/STAT3 in liver regeneration have been reported previously.[7,8,10,12,13,39]

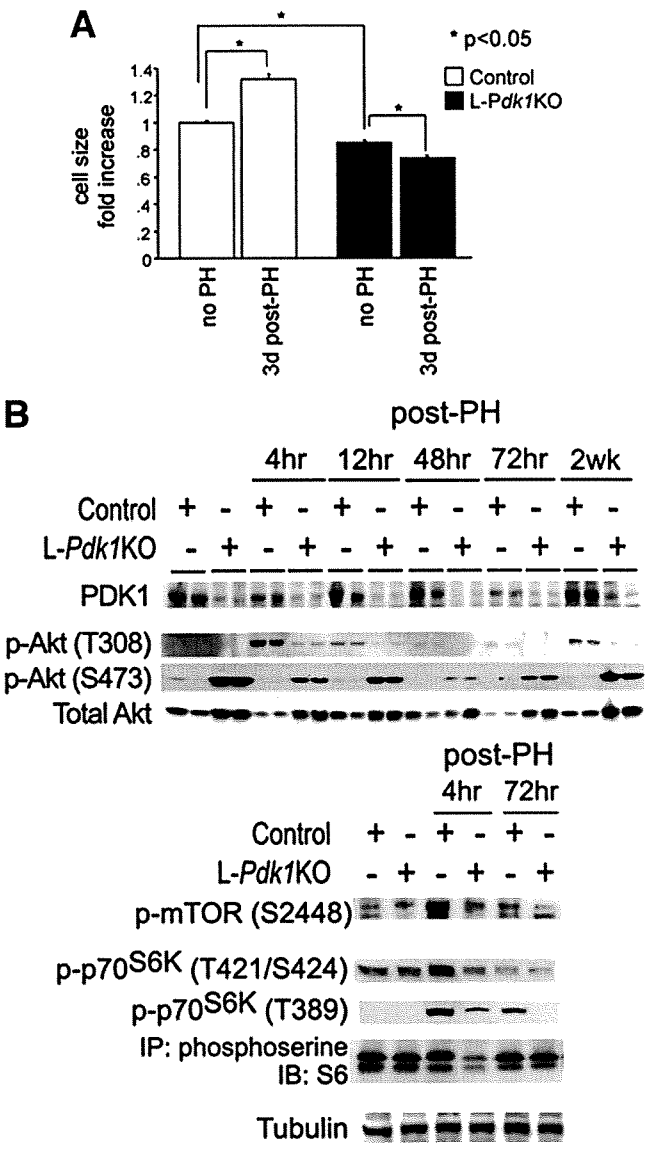

Fig. 4. Post-PH cell growth and activation of Akt, mTOR, p70^{S6K}, and S6 proteins in control and L-*Pdk1*KO liver (A, B). Responsive cell growth did not occur after PH in L-*Pdk1*KO mice. Akt, mTOR, p70^{S6K}, and S6 were all activated by PH in control mice, but hardly at all in L-*Pdk1*KO mice. The data at each time point consist of two representative blots from at least three independent experiments.

However, deletion of STAT3 in liver fails to affect liver regeneration despite almost completely suppressing the mitotic response, where Akt, p70^{S6K}, and mTOR signals are markedly activated.[6] It has therefore been suggested that "survival signals" such as Akt, p70^{S6K}, and mTOR may be responsible for the acute response in post-PH liver regeneration, possibly by regulating cell growth and thus may contribute to the initiation and maintenance of liver regeneration when the mitotic response is impaired.[6] Conversely, p70^{S6K}/S6, for example, is suggested to be involved in cell proliferation[40-42] and post-PH liver regeneration.[42] So far, the involvement and the roles of these

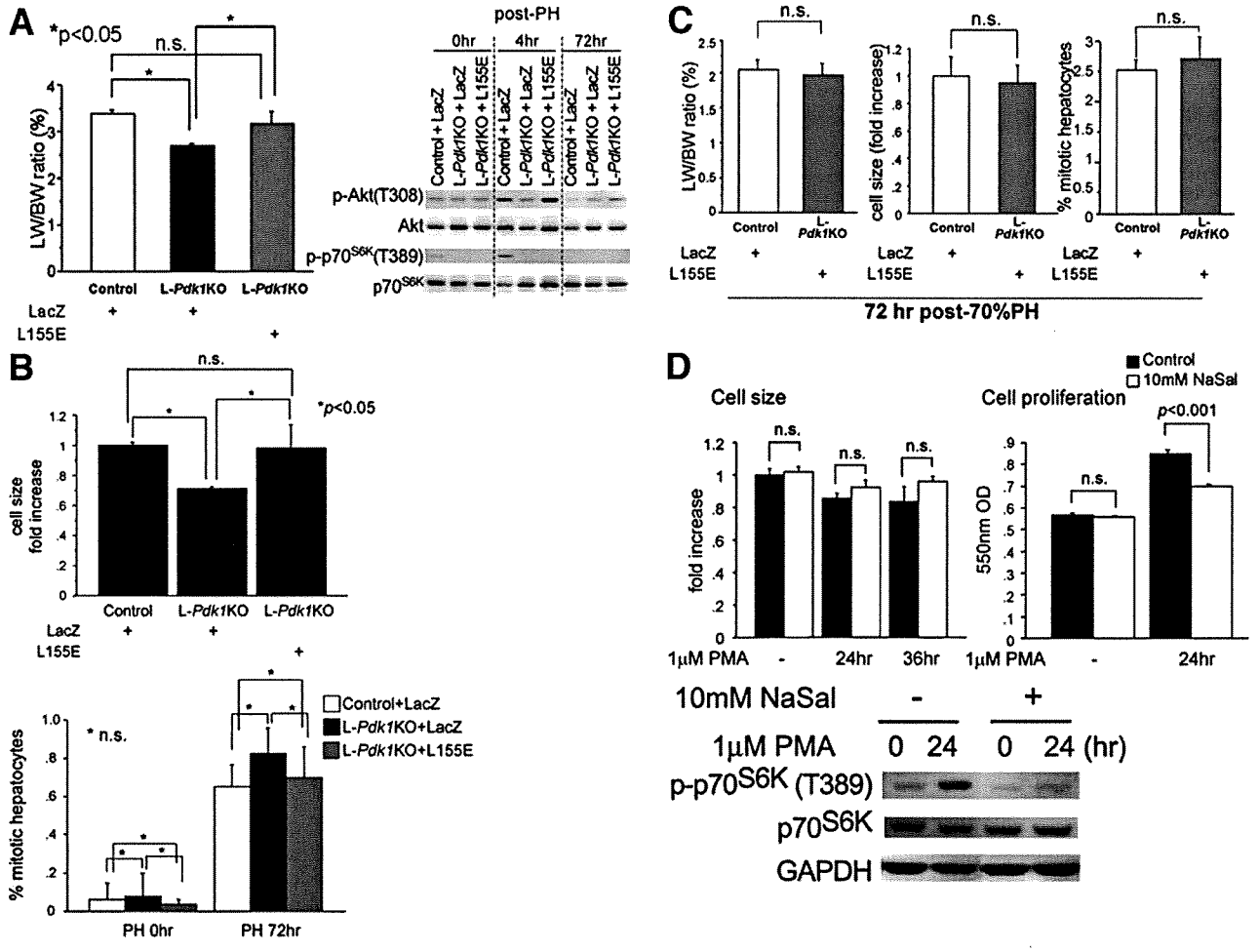

Fig. 5. Effects of Akt and p70^{S6K} on cell growth or proliferation in liver regeneration. (A) Introduction of pif-pocket mutant of PDK1 (L155E) to L-*Pdk1*KO liver allowed re-phosphorylation of Akt (Thr308), but not p70^{S6K} (Thr389), and normal regeneration of L-*Pdk1*KO liver 72 hours post-PH. (B) By introducing pif-pocket of PDK1 (L155E) into PDK1-deficient livers, hepatocytes re-grow in size, but post-PH mitotic cell counts are not affected. (C) Introduction of pif-pocket mutant of PDK1 (L155E) to L-*Pdk1*KO improved liver regeneration even in the 70% PH model. (D) Phosphorylation of p70^{S6K} (Thr389) suppressed by sodium salicylate (NaSal), an inhibitor of p70^{S6K} phosphorylation, in phorbol myristate acetate (PMA)-stimulated AML12 cells. NaSal was added to the culture media 16 hours before the experiment, and then AML12 cells were stimulated by PMA for 1 hour. Inhibition did not affect cell size, but slightly suppressed cell proliferation in phorbol myristate acetate-stimulated AML12 cells. Data are means ± SEM. Each blot is representative of at least three independent experiments.

proteins in cell proliferation and cell growth in liver regeneration have not been well delineated. In the current study, we investigated the roles of PI3-K/PDK1-mediated signaling pathways in liver regeneration after PH from the perspective of cell growth and proliferation. PI3-K signaled STAT3 for cell proliferation and PDK1/Akt for cell growth. We propose that PDK1/Akt-mediated signals (but not p70^{S6K}/S6) are essential contributors to physical and functional liver regeneration mainly by regulating cell size, but not cell proliferation.

PDK1-deficiency in liver had a critical effect on both physical and functional post-PH liver regeneration. Seventy percent PH was lethal to L-*Pdk1*KO mice; remaining liver tissue did not regenerate in either 70% or 30% PH models in L-*Pdk1*KO mice despite normal cell proliferation. The increase of cell size (cell growth) that occurred after PH in control mice was completely absent in L-*Pdk1*KO mice and in fact was even reduced (Fig. 4A). This finding may account for the impaired liver regeneration in L-*Pdk1*KO mice.

Regarding the molecules downstream of PDK1, Akt and mTOR were very weakly phosphorylated at quiescence, whereas they were markedly phosphorylated 4 hours after PH. In L-*Pdk1* KO mice, phosphorylation of these molecules was significantly reduced. In contrast, S6 (and p70^{S6K}) were phosphorylated even at quiescence in control mice, were phosphorylated 4 hours after PH, and had recovered to pre-PH levels by 72 hours post-PH. In L-*Pdk1* KO mice, phosphorylation of S6 was suppressed 4 hours after PH but recovered to pre-PH levels despite lack of recovery of liver mass. Considering these findings, it seems that PDK1 signals weakly to Akt/mTOR under

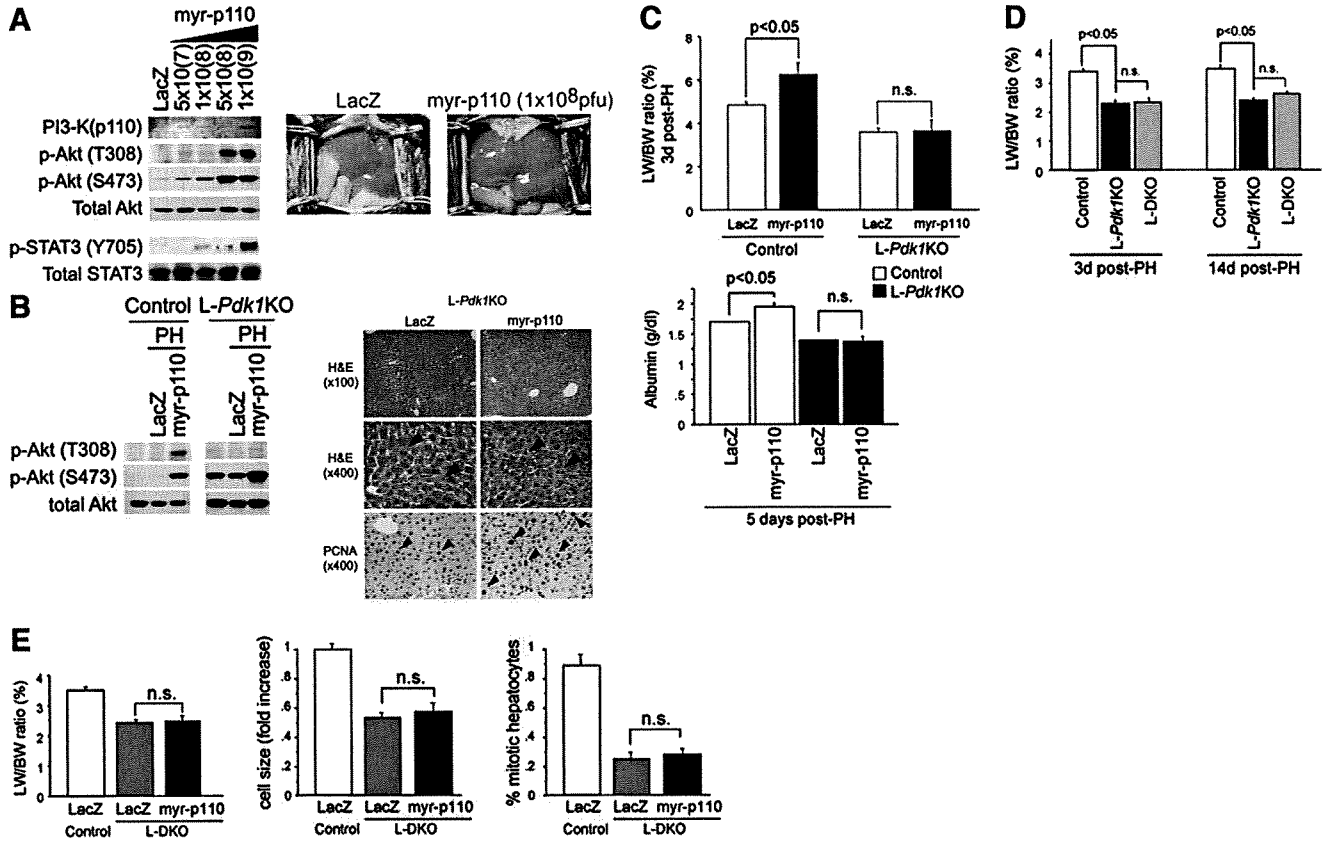

Fig. 6. Effects of PI3-K on liver regeneration in L-*Pdk1*KO mice. (A) Expression of constitutively active PI3-K (myr-p110) induced phosphorylation of Akt (Thr308 and Ser473) and STAT3 (Tyr705) in the liver and enlarged the liver mass. The amount of adenovirus was adjusted to 1×10^9 plaque-forming units in total by adding LacZ in each mouse. (B) Expression of constitutively active PI3-K (myr-p110) did not phosphorylate Akt at Thr308 and more strongly at Ser473 72 hours post-PH in L-Pdk1KO liver, and induced more hepatocyte proliferation after PH in L-*Pdk1*KO mice (Hematoxylin-eosin staining and immunostaining for PCNA. Arrowheads indicate mitotic hepatocytes. Original magnification ×200). (C) Activation of PI3-K failed to regenerate L-*Pdk1*KO liver after PH, despite efficacy in control liver. It also increased serum albumin levels in control mice, but not in L-*Pdk1*KO mice. Adenovirus vector encoding myr-p110 was intravenously injected at the time of surgery in this experiment (1×10^8 plaque-forming units/body). (D) Additional deletion of STAT3 in PDK1-deficient liver (L-DKO mice) did not further exacerbate liver regeneration in L-*Pdk1*KO mice. (E) Rescue experiment using myr-p110 showed that activation of PI3-K did not affect post-PH cell size, mitosis, or liver regeneration in L-DKO mice.

quiescent conditions but signals strongly immediately after PH in a transient manner for the liver regeneration response. In contrast, S6 (and $p70^{S6K}$) may be phosphorylated even when PDK1/$p70^{S6K}$ signals are not fully activated. S6 was phosphorylated after PH but returned to pre-PH levels regardless of liver mass recovery. These dynamics of protein phosphorylation may indicate that PDK1/Akt is more responsive than $p70^{S6K}$ to PH and plays more roles in liver regeneration. Canceling PDK1-mediated signals other than Akt in L-*Pdk1*KO liver led to full recovery of liver mass and responsive cell growth after PH. These findings suggest that PDK1/$p70^{S6K}$ signals may not be directly involved in cell growth–associated liver regeneration.

Stimulation of PI3-K induced activation of STAT3 and Akt, which enlarged liver and increased levels of serum albumin. This, however, failed to regenerate post-PH liver physically and functionally in L-*Pdk1*KO mice, despite marked proliferation of hepatocytes (Fig. 6B, C). Furthermore, liver regeneration of *Pdk1*KO and DKO mice was equally suppressed after PH (Fig. 6D). These findings clearly indicate the potential importance of PDK1 and PDK1-mediated cell growth in liver regeneration but suggest that STAT3-mediated cell proliferation is not involved. It was reported previously that Akt and associated signals are strongly activated immediately after PH in L-*Stat3*KO mice, in which the post-PH mitotic response is greatly suppressed,[6] and it was suggested that activation of these signals may be responsible for compensation of the impaired liver regeneration. Recent evidence indicates an essential role of certain molecules in determining cell size in genetically manipulated animals. Akt, mTOR, $p70^{S6K}$, and glycogen synthase kinase-3β are all good candidates for determining the original (inborn) cell size in various cells or organs.[19-21,23] This is consistent with our proposal that PDK1/Akt and associ-

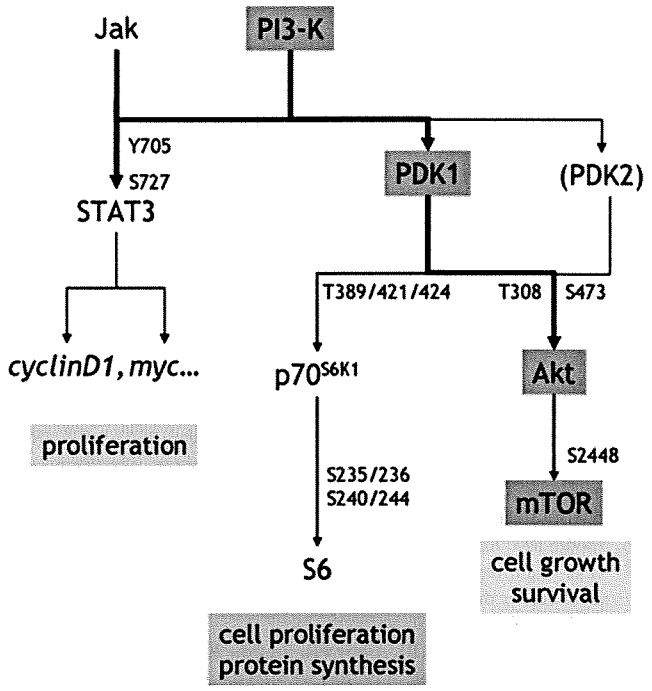

Fig. 7. Schematic illustration of the pivotal signaling pathways in liver regeneration. Janus kinase and PI3-K signaling to STAT3 for hepatocyte proliferation. PDK1/Akt plays a central role in cell growth-mediated liver regeneration and anti-apoptosis. $p70^{S6K}$ mediates protein synthesis and cell proliferation but may not be essential for liver regeneration.

ated signals contribute to liver regeneration mainly by inducing cell growth (cell size), but not by inducing cell proliferation.

Inhibition of $p70^{S6K}$ by salicylic acid mildly suppressed hepatocyte proliferation, although it was not seen to be involved in cell growth *in vitro* (Fig. 5C). It has been reported that $p70^{S6K}$/S6 deletion suppresses cell proliferation in different types of cells,[40-42] consistent with our results *in vitro*. However, hepatic suppression of $p70^{S6K}$ by deletion of PDK1 did not suppress hepatocyte proliferation after PH. Because PI3-K/STAT3 mitotic signals possibly function well enough to initiate/maintain cell proliferation in the post-PH liver, inhibition of $p70^{S6K}$ may not affect post-PH hepatocyte proliferation. Interestingly, mitotic responses and STAT3 activation after PH occurred to the same degree in L-*Pdk1*KO and control mice (Fig. 3A-D), despite the marked difference in liver regeneration (Fig. 2A, B). This indicates that, at least in the impaired liver regeneration induced by deficient PDK1, the interleukin-6/STAT3 pathway is activated but not sufficient to maintain normal liver regeneration.

Seventy percent PH was lethal in L-*Pdk1*KO mice (Fig. 2A) but not in L-*Stat3*KO mice.[6] Most L-*Pdk1*KO mice died within 12 hours of PH with no signs of liver regeneration. Serum markers of liver damage (glutamic oxaloacetic transaminase/glutamate pyruvate transaminase/lactate dehydrogenase and bilirubin) were moderately elevated 72 hours after PH even in 30% PH L-*Pdk1*KO mice (Fig. 2D), suggesting the possibility of post-PH extended liver failure in 70% PH L-*Pdk1*KO mice. The exact cause of death is not yet clear; however, remaining liver function certainly seems responsible for any survival. Liver function assessed by serum albumin level showed persistent reduction 14 days after PH. Reduced liver function of L-*Pdk1*KO mice may therefore be one of the major causes of death.

In conclusion, we have demonstrated a pivotal role for PDK1/Akt-mediated acute responsive cell growth in liver regeneration, and for PI3-K/STAT3-mediated mitotic pathway in a rodent PH model (Fig. 7). PDK1/Akt signals are especially crucial for avoiding post-PH liver failure as well as for maintaining normal liver regeneration capacity. Although further studies are necessary, the current report has begun to elucidate the molecular mechanisms underlying liver regeneration.

References

1. Michalopoulos GK, DeFrances MC. Liver regeneration. Science 1997; 276:60-66.
2. Fausto N. Liver regeneration: from laboratory to clinic. Liver Transpl 2001;7:835-844.
3. Kellersmann R, Gassel HJ, Buhler C, Thiede A, Timmermann W. Application of Molecular Adsorbent Recirculating System in patients with severe liver failure after hepatic resection or transplantation: initial single-centre experiences. Liver 2002;22(Suppl 2):56-58.
4. Shirabe K, Shimada M, Gion T, Hasegawa H, Takenaka K, Utsunomiya T, et al. Postoperative liver failure after major hepatic resection for hepatocellular carcinoma in the modern era with special reference to remnant liver volume. J Am Coll Surg 1999;188:304-309.
5. Topal B, Kaufman L, Aerts R, Penninckx F. Patterns of failure following curative resection of colorectal liver metastases. Eur J Surg Oncol 2003;29: 248-253.
6. Haga S, Ogawa W, Inoue H, Terui K, Ogino T, Igarashi R, et al. Compensatory recovery of liver mass by Akt-mediated hepatocellular hypertrophy in liver-specific STAT3-deficient mice. J Hepatol 2005;43:799-807.
7. Fausto N, Campbell JS, Riehle KJ. Liver regeneration. HEPATOLOGY 2006; 43:S45-S53.
8. Terui K, Ozaki M. The role of STAT3 in liver regeneration. Drugs Today (Barc) 2005;41:461-469.
9. Michalopoulos GK, DeFrances M. Liver regeneration. Adv Biochem Eng Biotechnol 2005;93:101-134.
10. Taub R. Liver regeneration: from myth to mechanism. Nat Rev Mol Cell Biol 2004;5:836-847.
11. Fausto N. Liver regeneration and repair: hepatocytes, progenitor cells, and stem cells. HEPATOLOGY 2004;39:1477-1487.
12. Cressman DE, Greenbaum LE, DeAngelis RA, Ciliberto G, Furth EE, Poli V, et al. Liver failure and defective hepatocyte regeneration in interleukin-6-deficient mice. Science 1996;274:1379-1383.
13. Taub R, Greenbaum LE, Peng Y. Transcriptional regulatory signals define cytokine-dependent and -independent pathways in liver regeneration. Semin Liver Dis 1999;19:117-127.
14. Ozaki M, Haga S, Zhang HQ, Irani K, Suzuki S. Inhibition of hypoxia/reoxygenation-induced oxidative stress in HGF-stimulated antiapoptotic signaling: role of PI3-K and Akt kinase upon rac1. Cell Death Differ 2003;10:508-515.

15. Conery AR, Cao Y, Thompson EA, Townsend CM, Ko TC, Luo K. Akt interacts directly with Smad3 to regulate the sensitivity to TGF-beta induced apoptosis. Nat Cell Biol 2004;6:366-372.
16. Gardai SJ, Hildeman DA, Frankel SK, Whitlock BB, Frasch SC, Borregaard N, et al. Phosphorylation of Bax Ser184 by Akt regulates its activity and apoptosis in neutrophils. J Biol Chem 2004;279:21085-21095.
17. Tanaka Y, Gavrielides MV, Mitsuuchi Y, Fujii T, Kazanietz MG. Protein kinase C promotes apoptosis in LNCaP prostate cancer cells through activation of p38 MAPK and inhibition of the Akt survival pathway. J Biol Chem 2003;278:33753-33762.
18. Lu Y, Parkyn L, Otterbein LE, Kureishi Y, Walsh K, Ray A, et al. Activated Akt protects the lung from oxidant-induced injury and delays death of mice. J Exp Med 2001;193:545-549.
19. Edinger AL, Thompson CB. Akt maintains cell size and survival by increasing mTOR-dependent nutrient uptake. Mol Biol Cell 2002;13:2276-2288.
20. Faridi J, Fawcett J, Wang L, Roth RA. Akt promotes increased mammalian cell size by stimulating protein synthesis and inhibiting protein degradation. Am J Physiol Endocrinol Metab 2003;285:E964-E972.
21. Latronico MV, Costinean S, Lavitrano ML, Peschle C, Condorelli G. Regulation of cell size and contractile function by AKT in cardiomyocytes. Ann N Y Acad Sci 2004;1015:250-260.
22. G-Amlak M, Uddin S, Mahmud D, Damacela I, Lavelle D, Ahmed M, et al. Regulation of myeloma cell growth through Akt/Gsk3/forkhead signaling pathway. Biochem Biophys Res Commun 2002;297:760-764.
23. Mourani PM, Garl PJ, Wenzlau JM, Carpenter TC, Stenmark KR, Weiser-Evans MC. Unique, highly proliferative growth phenotype expressed by embryonic and neointimal smooth muscle cells is driven by constitutive Akt, mTOR, and p70S6K signaling and is actively repressed by PTEN. Circulation 2004;109:1299-1306.
24. Pende M, Kozma SC, Jaquet M, Oorschot V, Burcelin R, Le Marchand-Brustel Y, et al. Hypoinsulinaemia, glucose intolerance and diminished beta-cell size in S6K1-deficient mice. Nature 2000;408:994-997.
25. Stiles B, Wang Y, Stahl A, Bassilian S, Lee WP, Kim YJ, et al. Liver-specific deletion of negative regulator Pten results in fatty liver and insulin hypersensitivity [corrected]. Proc Natl Acad Sci U S A 2004;101:2082-2087.
26. Inoue H, Ogawa W, Ozaki M, Haga S, Matsumoto M, Furukawa K, et al. Role of STAT-3 in regulation of hepatic gluconeogenic genes and carbohydrate metabolism in vivo. Nat Med 2004;10:168-174.
27. Mora A, Lipina C, Tronche F, Sutherland C, Alessi DR. Deficiency of PDK1 in liver results in glucose intolerance, impairment of insulin-regulated gene expression and liver failure. Biochem J 2005;385:639-648.
28. Inoue H, Ogawa W, Asakawa A, Okamoto Y, Nishizawa A, Matsumoto M, et al. Role of hepatic STAT3 in brain-insulin action on hepatic glucose production. Cell Metab 2006;3:267-275.
29. Yakar S, Liu JL, Stannard B, Butler A, Accili D, Sauer B, et al. Normal growth and development in the absence of hepatic insulin-like growth factor I. Proc Natl Acad Sci U S A 1999;96:7324-7329.
30. Collins BJ, Deak M, Arthur JS, Armit LJ, Alessi DR. In vivo role of the PIF-binding docking site of PDK1 defined by knock-in mutation. EMBO J 2003;22:4202-4211.
31. Kitamura T, Kitamura Y, Kuroda S, Hino Y, Ando M, Kotani K, et al. Insulin-induced phosphorylation and activation of cyclic nucleotide phosphodiesterase 3B by the serine-threonine kinase Akt. Mol Cell Biol 1999; 19:6286-6296.
32. Kawano F, Matsuoka Y, Oke Y, Higo Y, Terada M, Wang XD, et al. Role(s) of nucleoli and phosphorylation of ribosomal protein S6 and/or HSP27 in the regulation of muscle mass. Am J Physiol Cell Physiol 2007; 293:C35-C44.
33. Aguilar V, Alliouachene S, Sotiropoulos A, Sobering A, Athea Y, Djouadi F, et al. S6 kinase deletion suppresses muscle growth adaptations to nutrient availability by activating AMP kinase. Cell Metab 2007;5:476-487.
34. Biondi RM, Kieloch A, Currie RA, Deak M, Alessi DR. The PIF-binding pocket in PDK1 is essential for activation of S6K and SGK, but not PKB. EMBO J 2001;20:4380-4390.
35. Biondi RM, Komander D, Thomas CC, Lizcano JM, Deak M, Alessi DR, et al. High resolution crystal structure of the human PDK1 catalytic domain defines the regulatory phosphopeptide docking site. EMBO J 2002; 21:4219-4228.
36. McManus EJ, Collins BJ, Ashby PR, Prescott AR, Murray-Tait V, Armit LJ, et al. The in vivo role of PtdIns(3,4,5)P3 binding to PDK1 PH domain defined by knockin mutation. EMBO J 2004;23:2071-2082.
37. Law BK, Waltner-Law ME, Entingh AJ, Chytil A, Aakre ME, Nørgaard P, et al. Salicylate-induced growth arrest is associated with inhibition of p70s6k and down-regulation of c-myc, cyclin D1, cyclin A, and proliferating cell nuclear antigen. J Biol Chem 2000;275:38261-38267.
38. Liu JL, Mao Z, LaFortune TA, Alonso MM, Gallick GE, Fueyo J, et al. Cell cycle-dependent nuclear export of phosphatase and tensin homologue tumor suppressor is regulated by the phosphoinositide-3-kinase signaling cascade. Cancer Res 2007;67:11054-11063.
39. Fausto N. Liver regeneration. J Hepatol 2000;32:19-31.
40. Viñals F, Chambard JC, Pouysségur J. p70 S6 kinase-mediated protein synthesis is a critical step for vascular endothelial cell proliferation. J Biol Chem 1999;274:26776-26782.
41. Gäbele E, Reif S, Tsukada S, Bataller R, Yata Y, Morris T, et al. The role of p70S6K in hepatic stellate cell collagen gene expression and cell proliferation. J Biol Chem 2005;280:13374-13382.
42. Volarevic S, Stewart MJ, Ledermann B, Zilberman F, Terracciano L, Montini E, et al. Proliferation, but not growth, blocked by conditional deletion of 40S ribosomal protein S6. Science 2000;288:2045-2047.

Low prevalence of juvenile-onset Behçet's disease with uveitis in East/South Asian people

N Kitaichi, A Miyazaki, M R Stanford, et al.

Br J Ophthalmol 2009 93: 1428-1430 originally published online August 9, 2009
doi: 10.1136/bjo.2008.154476

Low prevalence of juvenile-onset Behçet's disease with uveitis in East/South Asian people

N Kitaichi,[1] A Miyazaki,[1] M R Stanford,[2] D Iwata,[1] H Chams,[3] S Ohno[1,4]

[1] Department of Ophthalmology and Visual Sciences, Hokkaido University Graduate School of Medicine, Sapporo, Japan; [2] King's College London, London, UK; [3] Behçet's Research Center, Shariati Hospital, Teheran University for Medical Sciences, Teheran, Iran; [4] Department of Ocular Inflammation and Immunology, Hokkaido University Graduate School of Medicine, Sapporo, Japan

Correspondence to:
Dr N Kitaichi, Department of Ophthalmology and Visual Sciences, Hokkaido University Graduate School of Medicine, Kita-15, Nishi-7, Kita-ku, Sapporo 060-8638, Japan;
nobukita@med.hokudai.ac.jp

Accepted 24 April 2009
Published Online First
9 August 2009

ABSTRACT

Aim: There is little information on the demographic and clinical characteristics of Behçet's disease in children in different parts of the world. We sought to provide this information through a questionnaire survey of specialist eye centres.

Methods: Descriptive questionnaires were collected from 25 eye centres in 14 countries. The questionnaire surveyed details of juvenile-onset Behçet's disease with uveitis. Ethnic groups, clinical features, treatments and prognosis of paediatric-age Behçet's disease were examined on a worldwide scale.

Results: The clinical data of 135 juvenile-onset and 1227 adult-onset patients with uveitis were collected. The average age of disease diagnosis in the children was 11.7 years old. Of the ethnic groups identified 54% were from Middle East, 43% from Europe, but only 2% from East/South Asian countries. By contrast, 19.2% of adult patients were from East or South Asia. The frequency of genital ulcers in juvenile patients was 38.7%, which was significantly lower than in adult cases (53.5%; $p<0.01$).

Conclusions: Behçet's disease with uveitis was less common in children than in adults in East/South Asia. Although the clinical features of the systemic disease were similar in children and adults, there was a lower frequency of genital ulceration in children.

Behçet's disease is a chronic multisystem disorder characterised by oral aphthous ulcers, genital ulcers, skin lesions, ocular lesions, gastrointestinal involvement, vascular lesions and neurological manifestations. The mean age of disease onset is 25–30 years old,[1] and initial presentation in children is uncommon. Details of the presentation and clinical characteristics of juvenile-onset Behçet's disease have been limited to case reports or small case series.[2–8]

One of the manifestations of Behçet's disease is uveitis. In general, uveitis in childhood is uncommon with an incidence of 4–7/100 000 children per year.[9–11] Unlike adults, juvenile idiopathic arthritis (JIA) is the most common identified cause of uveitis in children.[12–14] Even in Turkey, one of the countries of the highest prevalence of Behçet's disease, JIA is the most common cause of uveitis in children, followed by idiopathic uveitis and pars planitis.[15] Behçet's disease is one of the three most frequent diagnoses in patients with uveitis in Japan.[16–18] Although the prevalence of Behçet's disease in the Japanese population overall has been estimated to be 10–15/100 000,[19] juvenile-onset Behçet's disease is uncommon.

Accordingly, there is little information on the demography and clinical characteristics of Behçet's disease with ocular lesions in children. Against this background, we administered a descriptive questionnaire survey in a large-scale international collaborative study and compared the epidemiology, clinical phenotype and visual outcome in children and adults. A summary of the clinical features of the whole cohort has been recently reported.[1]

METHODS

Descriptive questionnaires were sent to 132 ophthalmology centres by email and airmail in 2005–2006. We encouraged the centres to provide clinical data on as many patients as possible. We gave no details of juvenile-onset Behçet's disease in the survey to avoid bias in the recruitment of patients in their institutions. Responses were collected from 25 eye centres in 14 countries; Australia, Germany, Greece, India, Iran, Italy, Japan, Jordan, Morocco, Portugal, Turkey, Saudi Arabia, Tunisia and the UK. The race of each patient was also ascertained. The inclusion criterion was development of the disease at less than 16 years of age. The age of disease onset was recognised as the timing of meeting the classification criteria based on the estimation of the responding doctors. Statistical analysis was performed using the χ^2 test or F test. Values of $p<0.01$ were considered statistically significant.

RESULTS

Clinical data on 1465 Behçet's disease patients were successfully collected. From these, the age of disease onset was reported for 1362 patients: 1227 patients were considered adult-onset and 135 were juvenile-onset. Boys accounted for 65.2% of the cohort of juvenile-onset patients (table 1). HLA-B51 was detected in 68.6% of children and 61.6% of adult patients. The mean age of disease diagnosis in children was 11.7 years old, and the mean follow-up period was 13.5 years (table 1). We were able to identify the ethnic groups of 127 children: 53.5% (68 cases) were from Middle Eastern countries, 43.3% (55 cases) from Europe, and only 2.4% (three cases) from East/South Asia (fig. 1). One case was reported as Cuban of mixed race. Among adults, 19.2% of patients were from East/South Asia (fig. 1). This difference in ethnicity was significantly different between adult-onset and juvenile-onset ($p<0.004$, F test).

Among children, there were recurrent oral aphthous ulcers in 94.8%, skin lesions in 67.4% and genital ulcers in 38.5% (fig. 2). In adults, recurrent oral aphthous ulcers in 94.5%, skin lesions in 70.0% and genital ulcers in 53.5% (fig. 2). The frequency of genital ulcers in juvenile patients was significantly lower than that in adult

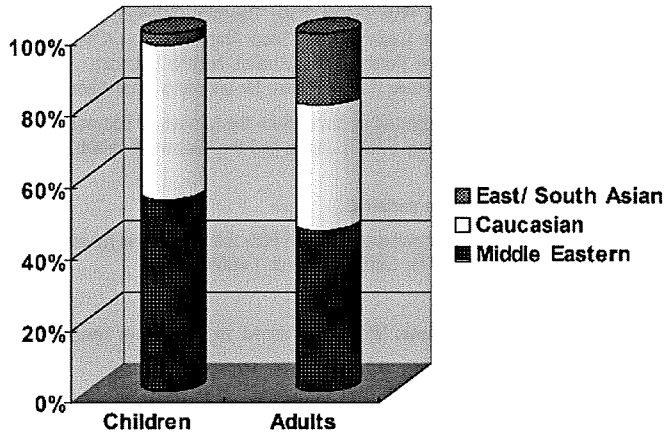

Figure 1 Ethnic groups of patients with Behçet's disease. Middle Eastern, Caucasian and East/South Asian people were the three major ethnic groups of Behçet's disease among adults. However, only a few East/South Asian patients suffered from the disease in childhood ($p<0.01$).

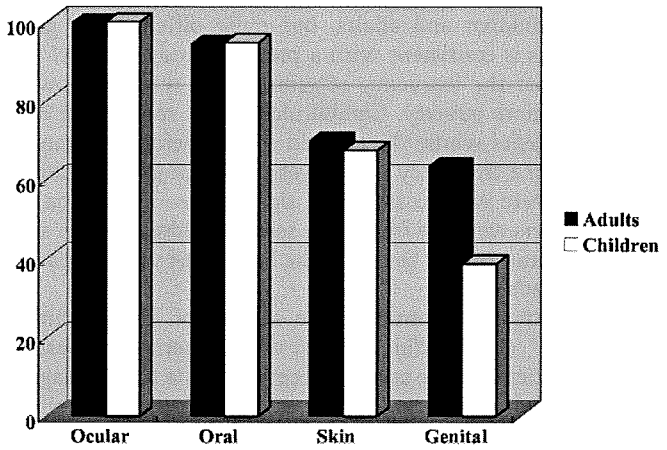

Figure 2 Frequency (%) of the major symptoms of Behçet's disease. The frequency of genital ulcers was significantly lower in children than in adults ($p<0.01$).

cases ($p<1\times10^{-8}$, χ^2 test). More than 90% (93.9%) of juvenile patients developed combined anterior and posterior segment intraocular inflammation (CAPSII)/panuveitis as adults. Most of the children suffered from bilateral recurrent CAPSII/panuveitis (table 1). The percentage of eyes achieving a final visual acuity of 0.1 (20/200) or better in the better eye was 92.6% of children (table 1) and 86.3% of adults. Thus, 7.4% of children but 13.7% of adult patients were legally blind. A good visual prognosis (≥20/200) was more frequent in children than in adult cases ($p<0.033$, χ^2 test).

The most frequently prescribed systemic therapy was corticosteroids (57 cases, 42.2%), followed by cyclophosphamide (27 cases, 20.0%), methotrexate (25 cases, 18.5%), colchicine (18 cases, 13.3%), azathioprine (12 cases, 8.9%), ciclosporin (11 cases, 8.1%) and interferon-α (two cases, 1.5%) (table 2). Three-quarters (73.6%) of patients received more than one drug.

DISCUSSION

In the present study, we successfully performed an international collaborative survey of the phenotypes of children with Behçet's disease and uveitis. Although several diagnostic criteria are used to make the diagnosis of Behçet's disease in adults,[20 21] there are no diagnostic criteria in children.[22] This means that the epidemiology of paediatric Behçet's disease is difficult to evaluate because there is no general agreement about either the age of onset or the age of full diagnosis. Previous studies have shown that the proportion of patients in whom the onset of symptoms occurred under the age of 16 years varies.[3 23 24] A study of juvenile-onset Behçet's disease from France reported that the mean age of disease onset was 7.5 years old, but the mean age at which patients met the criteria for Behçet's disease was 11.6 years old.[4] Since the mean age of disease diagnosis in our study was 11.7 years old (table 1), our present results from an international study confirm these previous findings.

We showed that the visual prognosis was better in juvenile-onset patients than in adult-onset subjects. More than 20% of eyes of Behçet's patients of all ages become legally blind as reported recently.[1 25] In the present study, 93% of the juvenile patients had final visual acuity of 0.1 (20/200) or better in their better eyes (table 1), and visual prognosis was significantly better among children than adults. However, this statistical result may not always mean that the ocular involvement in children is milder than adults. The visual prognosis of patients from East/South Asia was poor compared with other countries in all age groups, as we reported.[1] In addition, the prevalence in East/South Asia was significantly lower than that in the Middle East and European countries (fig 1). Thus, only a few East/South Asian children, a group with a poor visual prognosis, were included in the population of the present study. Furthermore, we did not have information on ocular co-morbidity (eg cataract, glaucoma and/or macular degeneration) as a confounding factor, which might be expected to be more common in adults. It should be noted that cyclophosphamide was one of the most commonly used immunosuppressive agents in this study. Although it is true that this old drug is cheap and familiar in many countries, it is not recommended for children because of its toxicity.

Table 1 Summary of juvenile-onset Behçet's disease in eye centres (n = 135)

Variable	Incidence (%)
Boys	65.5
HLA-B51	68.6
Age of disease onset	11.7*
Mean follow-up period	13.5*
CAPSII/panuveitis	93.9
Bilaterality	83.6
Recurrence of ocular inflammation	96.3
Poor visual prognosis (<20/200, better eyes)	7.4

CAPSII, combined anterior and posterior segment intraocular inflammation.
*Years.

Table 2 Initial systemic therapies for children

Treatment	%
Corticosteroids	42.2
Cyclophosphamide	20.0
Methotrexate	18.5
Colchicine	13.3
Azathioprine	8.9
Ciclosporin	8.1
Interferon-α	1.5

Three-quarters of patients received two or more drugs as their initial therapies.

The prevalence of oral and skin lesions were almost the same between children and adults, but quite different for genital ulcers. This is consistent with a previous study in Israel.[6] It is possible that the frequency of genital ulcer might be lower in patients before puberty. Genital ulcers were reported in 30.9% of the patients whose disease had started before 10 years old. Although the frequency was lower than that of older children (42.7%), there was no statistical significance. The reason why genital ulcers were less frequently seen in children than in adults is still unclear. It may be one of the features of younger patients with Behçet's disease.

Our study may contain some sources of bias as outlined previously.[1] (1) We did not ask what criteria were used to include patients in the study. Accepted criteria for the diagnosis of Behçet's disease include those of the Japanese Committee,[21] the International Study Group[20] and O'Duffy.[26] The use of different standardised criteria may lead to misclassification when comparing the frequencies of systemic features. However, since most of the colleagues were members of International Committee of Behçet's Disease as well as uveitis specialists, the false-positive rate of diagnosis should be quite low. In addition, each had used the same criteria for inclusion of both juvenile and adult patients. (2) We also had only a limited response rate to the questionnaire from 25/132 eye centres. Therefore, the response may not have been representative of all countries and ethnic groups. (3) There may have been reporting bias as the population was taken from tertiary referral centres and the cases may have been more severe. (4) Access to uveitis clinic may be another source of bias. Healthcare systems are different in each country. There may be some regional problems relevant to the paediatric age group. However, in Japan, children can seek immediate medical attention, as can adults. This may partially explain the low prevalence of juvenile-onset Behçet's disease in East Asia. Japanese paediatricians previously monitoring Behçet's disease among children were able to collect the medical data of only 31 cases from 1290 hospitals throughout the country.[27] It may that the prevalence of the patients without ocular symptoms is also low in Japan.

Although there were some sources of bias that may distort the results, the authors consider that data from a sufficient number of patients with a relatively uncommon type of disease were analysed. The present results provide an indication that the clinical features of juvenile-onset Behçet's disease with ocular lesions do differ from adult-onset disease in some respects.

In conclusion, there were racial differences in the frequency of Behçet's disease in children. Only a few children suffered from Behçet's disease in contrast to the high prevalence in adults in East and South Asian. The clinical features of Behçet's disease with uveitis were different in adult-onset and juvenile-onset patients: the prevalence of genital ulcers was less in children than in adults.

Acknowledgements: The authors are grateful to Drs Krause (Berlin, Germany), Becker, Mackensen (Heidelberg, Germany), Forrester, Kuffova (Aberdeen, UK), Dick (Bristol, UK), Markomichelakis, Palimeris (Athens, Greek), Ozyazgan, Tugal-Tutkun (Istanbul, Turkey), Akova (Ankara, Turkey), de Abreu, Proenca (Evola, Portugal), Benamour (Casablanca, Morocco), Tognon, Motterle (Padova, Italy), Khairallah (Monastir, Tunisia), Accorinti, Pezzi (Rome, Italy), Davatchi (Teheran, Iran), Madanat (Amman, Jordan), Tabbara, al Dalaan (Ryadh, Saudi Arabia), Biswas (Chennai, India), Gupta (Chandigarh, India), Hall (Melbourne, Australia), Namba (Sapporo, Japan), and Okada, Kawaguchi and Mochizuki (Tokyo, Japan) for providing observational data.

Funding: This study was supported by grants from the Ministry of Education, Culture, Sports, Science and Technology (MEXT) Japan, and the Ministry of Health, Labor and Welfare Japan.

Competing interests: None declared.

Ethics approval: Ethics approval was obtained from the Institutional Review Board of Hokkaido University Hospital for Clinical Research (#009-0065).

Patient consent: Obtained.

Provenance and peer review: Not commissioned; externally peer reviewed.

REFERENCES

1. **Kitaichi N,** Miyazaki A, Iwata D, *et al*. Ocular features of Behcet's disease: an international collaborative study. *Br J Ophthalmol* 2007;**91**:1579–82.
2. **Jog S,** Patole S, Koh G, *et al*. Unusual presentation of neonatal Behcets disease. *Am J Perinatol* 2001;**18**:287–92.
3. **Kim DK,** Chang SN, Bang D, *et al*. Clinical analysis of 40 cases of childhood-onset Behcet's disease. *Pediatr Dermatol* 1994;**11**:95–101.
4. **Kone-Paut I,** Gorchakoff-Molinas A, Weschler B, *et al*. Paediatric Behcet's disease in France. *Ann Rheum Dis* 2002;**61**:655–6.
5. **Kone-Paut I,** Yurdakul S, Bahabri SA, *et al*. Clinical features of Behcet's disease in children: an international collaborative study of 86 cases. *J Pediatr* 1998;**132**:721–5.
6. **Krause I,** Uziel Y, Guedj D, *et al*. Childhood Behcet's disease: clinical features and comparison with adult-onset disease. *Rheumatology (Oxford)* 1999;**38**:457–62.
7. **Yamazaki S,** Koyano T. A case of pediatric Behcet's disease with intestinal involvement. *J Dermatol* 1999;**26**:160–3.
8. **Yazici H,** Tuzun Y, Pazarli H, *et al*. Influence of age of onset and patient's sex on the prevalence and severity of manifestations of Behcet's syndrome. *Ann Rheum Dis* 1984;**43**:783–9.
9. **Edelsten C,** Reddy MA, Stanford MR, *et al*. Visual loss associated with pediatric uveitis in english primary and referral centers. *Am J Ophthalmol* 2003;**135**:676–80.
10. **Gritz DC,** Wong IG. Incidence and prevalence of uveitis in Northern California; the Northern California Epidemiology of Uveitis Study. *Ophthalmology* 2004;**111**: 491–500.
11. **Paivonsalo-Hietanen T,** Tuominen J, Saari KM. Uveitis in children: population-based study in Finland. *Acta Ophthalmol Scand* 2000;**78**:84–8.
12. **Cunningham ET Jr.** Uveitis in children. *Ocul Immunol Inflamm* 2000;**8**:251–61.
13. **Kadayifcilar S,** Eldem B, Tumer B. Uveitis in childhood. *J Pediatr Ophthalmol Strabismus* 2003;**40**:335–40.
14. **Stoffel PB,** Sauvain MJ, von Vigier RO, *et al*. Non-infectious causes of uveitis in 70 Swiss children. *Acta Paediatr* 2000;**89**:955–8.
15. **Tugal-Tutkun I,** Havrlikova K, Power WJ, *et al*. Changing patterns in uveitis of childhood. *Ophthalmology* 1996;**103**:375–83.
16. **Akiyama K,** Numaga J, Yoshida A, *et al*. Statistical analysis of endogenous uveitis at Tokyo University Hospital (1998–2000). *Jpn J Ophthalmol* 2006;**50**:69–71.
17. **Goto H,** Mochizuki M, Yamaki K, *et al*. Epidemiological survey of intraocular inflammation in Japan. *Jpn J Ophthalmol* 2007;**51**:41–4.
18. **Kitamei H,** Kitaichi N, Namba K, *et al*. Clinical features of intraocular inflammation in Hokkaido, Japan. *Acta Ophthalmol* 2009;**87**:424–8.
19. **Kitaichi N,** Ohno S. [Behcet's disease]. *Nippon Rinsho* 2005;**63**(Suppl 5):376–80.
20. **ISGBD.** Criteria for diagnosis of Behcet's disease. International Study Group for Behcet's Disease. *Lancet* 1990;**335**:1078–80.
21. **Mizushima Y.** Recent research into Behcet's disease in Japan. *Int J Tissue React* 1988;**10**:59–65.
22. **Kitaichi N,** Ohno S. Behcet disease in children. *Int Ophthalmol Clin* 2008;**48**:87–91.
23. **Sarica R,** Azizlerli G, Kose A, *et al*. Juvenile Behcet's disease among 1784 Turkish Behcet's patients. *Int J Dermatol* 1996;**35**:109–11.
24. **Treudler R,** Orfanos CE, Zouboulis CC. Twenty-eight cases of juvenile-onset Adamantiades-Behcet disease in Germany. *Dermatology* 1999;**199**:15–9.
25. **Yang P,** Fang W, Meng Q, *et al*. Clinical features of Chinese patients with Behcet's disease. *Ophthalmology* 2008;**115**:312–18.
26. **D'Duffy J.** Criteres proposes pour le diagnostic de la maladie de Behcet's et notes therapeutiques. *Rev Med* 1994;**36**:2371–9.
27. **Fujikawa S,** Suemitsu T. Behcet disease in children: A nationwide retrospective survey in Japan. *Acta Paediatr Jpn* 1997;**39**:285–9.

Experimental Eye Research 90 (2010) 41–48

Contents lists available at ScienceDirect

Experimental Eye Research

journal homepage: www.elsevier.com/locate/yexer

Prevention of experimental autoimmune uveoretinitis by blockade of osteopontin with small interfering RNA☆

Daiju Iwata [a,b], Mizuki Kitamura [a,b], Nobuyoshi Kitaichi [b], Yoshinari Saito [c], Shigeyuki Kon [c], Kenichi Namba [b], Junko Morimoto [c], Akiko Ebihara [a,b], Hirokuni Kitamei [b], Kazuhiko Yoshida [b], Susumu Ishida [b], Shigeaki Ohno [d], Toshimitsu Uede [c], Kazunori Onoé [a], Kazuya Iwabuchi [a,d,*]

[a] Division of Immunobiology, Institute for Genetic Medicine, Hokkaido University, Kita-15, Nishi-7, Kita-ku, Sapporo 060-0815, Japan
[b] Department of Ophthalmology and Visual Sciences, Hokkaido University Graduate School of Medicine, Sapporo, Japan
[c] Division of Molecular Immunology, Institute for Genetic Medicine, Hokkaido University, Sapporo, Japan
[d] Department of Ocular Inflammation and Immunology, Hokkaido University Graduate School of Medicine, Sapporo, Japan

ARTICLE INFO

Article history:
Received 16 July 2008
Accepted in revised form
9 September 2009
Available online 18 September 2009

Keywords:
inflammation
EAU
OPN
RNA interference
uveitis

ABSTRACT

Osteopontin (OPN) is elevated during the progression of experimental autoimmune uveoretinitis (EAU) in C57BL/6 (B6) mice. Furthermore, EAU symptoms are ameliorated in OPN knockout mice or in B6 mice treated with anti-OPN antibody (M5). Recently, OPN has been shown to promote the Th1 response not only in the extracellular space as a secretory protein but also in cytosol as a signaling component. Thus, we attempted to reduce OPN in both compartments by using a small interfering RNA (siRNA) targeting the OPN coding sequence (OPN-siRNA). EAU was induced in B6 mice by immunization with human interphotoreceptor retinoid-binding protein (hIRBP) peptide sequence 1–20. The OPN- or control-siRNA was administered with hydrodynamic methods 24 h before and simultaneously with immunization (prevention regimen). When plasma OPN levels were quantified following siRNA administration with the prevention regimen, the level in the OPN-siRNA-treated group was significantly lower than that in the control-siRNA-treated group. Accordingly, the clinical and histopathological scores of EAU were significantly reduced in B6 mice when siRNA caused OPN blockade. Furthermore, TNF-α, IFN-γ, IL-2, GM-CSF and IL-17 levels in the culture supernatants were markedly suppressed in the OPN-siRNA-treated group, whereas the proliferative responses of T lymphocytes from regional lymph nodes against immunogenic peptides was not significantly reduced. On the other hand, the protection was not significant if the mice received the OPN-siRNA treatment on day 7 and day 8 after immunization when the clinical symptoms appeared overt (reversal regimen). Our results suggest that OPN blockade with OPN-siRNA can be an alternative choice for the usage of anti-OPN antibody and controlling uveoretinitis in the preventive regimen.

1. Introduction

Experimental autoimmune uveoretinitis (EAU) is an animal model of human endogenous uveoretinitis, including sympathetic ophthalmia, birdshot retinochoroidopathy, Vogt-Koyanagi-Harada's disease, and Behçet's disease (Caspi et al., 1988). EAU is induced by immunization with a retinal antigen (Ag), e.g., interphotoreceptor retinoid-binding protein (IRBP), or by the adoptive transfer of retinal Ag-specific T lymphocytes (Mochizuki et al., 1985; Caspi et al., 1986; Gregerson et al., 1986). EAU induced with immunization of retinal Ag now represents not only Th1 but also Th17-cell-mediated ocular diseases. A massive inflammatory infiltration composed primarily of mononuclear cells causes a rapid and irreversible destruction of photoreceptor cells (Jiang et al., 1999; Silver et al., 1999; Caspi, 2003; Amadi-Obi et al., 2007; Luger et al., 2008). It has been demonstrated that the augmentation of the Th2 response and T regulatory cytokine production and down-regulation of the Th1 response can mitigate inflammation and protect against the development of EAU (Saoudi et al., 1993; Kezuka et al., 1996; Caspi, 2002).

☆ This work was supported in part by a grant for Research on Behçet's Disease from The Ministry of Health, Labor, and Welfare Japan, by Grants-in-Aid for Scientific Research (S) and (C) from the Japan Society for the Promotion of Science (JSPS) and a Grant-in-Aid for Scientific Research on Priority Areas from The Ministry of Education, Culture, Sports, Science and Technology (MEXT) Japan. KI is also supported by the Global COE Program 'Establishment of International Collaboration Center for Zoonosis Control' from MEXT, and grants from The Suhara Memorial Foundation and Heisei Ijuku Tomakomai East Hospital.

* Corresponding author at: Division of Immunobiology, Institute for Genetic Medicine, Hokkaido University, Kita-15, Nishi-7, Kita-ku, Sapporo 060-0815, Japan. Tel.: +81 11 706 5532; fax: +81 11 706 7545.
E-mail address: akimari@igm.hokudai.ac.jp (K. Iwabuchi).

0014-4835/$ – see front matter © 2009 Elsevier Ltd. All rights reserved.
doi:10.1016/j.exer.2009.09.008

Osteopontin (OPN), also known as early T lymphocyte activation 1 (Eta-1), a secreted phosphoglycoprotein (SPP), contains the arginine-glycine-aspartic acid (RGD) integrin-binding sequence that is found in many extracellular matrix (ECM) proteins (O'Regan and Berman, 2000). OPN mediates adhesion and migration of a number of different cells types (O'Regan and Berman, 2000). OPN is widely produced by a variety of inflammatory cells, including T cells, macrophages, NK cells, and NKT cells (Denhardt et al., 2001; Diao et al., 2004, 2008) and induces interleukin-12 (IL-12) and IFN-γ production and inhibits IL-10 expression (Ashkar et al., 2000). Moreover, the intracellular isoform, OPN-i is now considered to promote the Th1 response through type I interferon production (Shinohara et al., 2006; Cantor and Shinohara, 2009). OPN has therefore been considered to act as a cytokine contributing to the development of Th1-mediated immunity and diseases and is anticipated to be a therapeutic target for controlling these diseases.

Indeed, recent studies, including ours, indicate that OPN possesses an aggravating role in EAU (Hikita et al., 2006; Kitamura et al., 2007), as had already been demonstrated in experimental autoimmune encephalomyelitis (EAE) (Ashkar et al., 2000; Chabas et al., 2001), anti-type II collagen antibody-induced arthritis (Yumoto et al., 2002; Yamamoto et al., 2003), and autoimmune hepatitis (Diao et al., 2004; Saito et al., 2007). Furthermore, we demonstrated that a specific antibody (M5) reacting to the SLAYGLR sequence, a newly exposed binding site, within OPN by thrombin cleavage, significantly suppressed clinical and histopathological scores of EAU in mice (Kitamura et al., 2007).

RNA interference (RNAi) is a powerful tool for silencing gene expression, by which double-stranded RNA (dsRNA) triggers the sequence-specific degradation of messenger RNA. In particular, small interfering RNAs (siRNAs), 21–23 nucleotide-length fragments (Elbashir et al., 2001; Hannon, 2002; Xie et al., 2006), have been shown to be of great value in decreasing the expression of the target gene by *in vivo* administration (Song et al., 2003; Nakamura et al., 2004; Schiffelers et al., 2005; Khoury et al., 2006).

In the present study, we applied siRNA targeting to an OPN coding sequence (OPN-siRNA) to inhibit OPN function by reducing OPN expression. We demonstrate the remarkable efficacy of OPN-siRNA to prevent EAU in mice.

2. Materials and methods

2.1. Experimental animals

6- to 8-week old female C57BL/6 (H-2^b; B6) mice were obtained from Japan SLC (Shizuoka, Japan). All studies were conducted in compliance with the Statement for the Use of Animals in Ophthalmic and Vision Research by the Association for Research in Vision and Ophthalmology (ARVO, Rockville, MD) and with the Hokkaido University Committee for Animal Use and Care.

2.2. Reagent

hIRBP (human interphotoreceptor retinoid-binding protein) peptide sequence 1–20 (GPTHLFQPSLVLDMAKVLLD) was purchased from Sigma-Genosys Japan (Ishikari City, Hokkaido, Japan). Purified *Bordetella pertussis* toxin (PTX) was purchased from Sigma–Aldrich (St. Louis, MO) and complete Freund's adjuvant (CFA) and *Mycobacterium tuberculosis* strain H37Ra were purchased from Difco (Detroit, MI).

2.3. Immunization

To analyze the cell proliferative response, $hIRBP_{1-20}$ (100 μg) was emulsified in CFA (1:1 v/v) and a total of 50 μl of the emulsion was injected subcutaneously (s.c.). To induce EAU, $hIRBP_{1-20}$ (200 μg) was emulsified in CFA (1:1 v/v) containing 2.5 mg/ml *M. tuberculosis* H37Ra. A total of 200 μl of the emulsion was injected s.c. concurrent with immunization, 0.1 μg of PTX in 100 μl phosphate-buffered saline (PBS) was injected intraperitoneally (i.p.) as an additional adjuvant (Kezuka et al., 1996).

2.4. Evaluation of EAU

Clinical assessment by funduscopic examination of the chorioretinal inflammation was carried out every 3 or 4 days from day 7 after immunization (Namba et al., 2000). The severity of EAU was graded 0–4 as described previously (Thurau et al., 1997). Briefly, the clinical scoring was based on vessel dilatation, the number of vessel white focal lesions, vessel white linear lesions and hemorrhages, and the extent of retinal detachment.

For the histological assessment of EAU, eyes were enucleated on day 21 after immunization. Removed eyes were fixed in 4% paraformaldehyde for an hour and transferred into 10% phosphate-buffered formaldehyde until processing. Fixed samples were embedded in paraffin and 5 μm sagittal sections were cut near the optic nerve head and stained with hematoxylin and eosin. The severity of EAU in each eye was scored on a scale of 0–4 as described previously (Caspi et al., 1988). In brief, no change was scored as 0. Focal non-granulomatous, monocytic infiltrations in the choroid, ciliary body, and retina were scored as 0.5. Retinal perivascular infiltration and monocytic infiltration in the vitreous were scored as 1. Granuloma formation in the uvea and retina, occluded retinal vasculitis, along with photoreceptor folds, serous retinal detachment, and loss of photoreceptors were scored as 2. In addition, the formation of granuloma at the level of the retinal pigmented epithelium and the development of subretinal neovascularization were scored as 3 and 4 according to the number and the size of the lesions.

2.5. Preparation of OPN- and control-siRNA

OPN- and control-siRNAs were purchased from B-Bridge (Sunnyvale, CA, USA). The sequences of sense and anti-sense strands of each siRNA were as follows: mouse OPN-RNAi-5/239: 5′-GCCAUGA CCACAUGGACGAdTdT-3′ (sense), 5′-UCGUCCAUGUGGUCAUGGCdT dT-3′ (anti-sense), control-siRNA pair, as designed to avoid specific sequences in mice; 5′-ACUCUAUCUGCACGCUGACUU-3′ (sense), 5′-GUCAGCGUGCAGAUAGAGUUU-3′ (anti-sense) (Saito et al., 2007). The siRNAs were deprotected, annealed and desalted.

2.6. In vivo treatment of mice with siRNA

Synthetic siRNAs were delivered *in vivo* using a modified hydrodynamic transfection method (Song et al., 2003), in which 50 μg of either OPN- or control-siRNA dissolved in 1 ml PBS was rapidly injected into the tail vein. Mice were treated with two injections of either OPN- or control-siRNA, 24 h before and simultaneously with the immunization (prevention regimen). Another group of mice was treated with two injections of either OPN- or control-siRNA on day 7 and day 8 after the immunization (reversal regimen).

2.7. Plasma OPN level

To quantify OPN concentration in plasma from EAU mice treated with either OPN-siRNA or control-siRNA, mice were deeply anesthetized with ether, and then blood was collected transcardially before immunization and on days 3, 7, 10, 14, 21, and 28 after immunization. All blood samples were collected in the presence of EDTA to avoid cleavage by thrombin *in vitro*, centrifuged to remove cells and debris, and stored at −80 °C. OPN concentration in plasma

samples (n = 24 mice) was quantified by an enzyme-linked immunosorbent assay (ELISA) kit for mouse OPN (Immuno-Biological Laboratories Co. Ltd., Takasaki, Japan) according to the manufacturer's protocol.

2.8. T cell proliferative responses

T cells obtained from B6 mice that had been primed with $hIRBP_{1-20}$ were cultured with Ag-presenting cells (APC) and $hIRBP_{1-20}$ as described elsewhere (Kitamura et al., 2007). In brief, T cell-enriched fraction was prepared as Nylon wool non-adherent cells by passing dispersed cells of draining lymph nodes from $hIRBP_{1-20}$-primed mice over nylon wool column. Then the T-enriched fraction (5×10^5/well) were co-cultured with mitomycin-C (MMC)-treated splenocytes as APC (5×10^5/well) and $hIRBP_{1-20}$ peptide at the indicated concentration in serum-free medium (RPMI 1640 medium), 10 mM Hepes, 0.1 mM non-essential amino acids, 1 mM sodium pyruvate, 50 μg/ml gentamicin sulfate, supplemented with 0.1% bovine serum albumin, and ITS + 1 liquid media supplement [2 μg/ml insulin from bovine pancreas, 1.1 μg/ml iron-free transferrin, 1 ng/ml sodium selenite, 100 μg/ml bovine serum albumin, and 1 μg/ml linoleic acid] (Sigma Chemical Co.). Cells in 96-well flat-bottomed plates were incubated for 64 h at 37 °C in 5% CO_2 in air, pulsed with 18.5 kBq of [^{3}H]-thymidine (Perkin Elmer Japan, Tokyo) per well during the last 16 h of incubation, and then were harvested. Incorporation of [^{3}H]-thymidine was quantified with a direct β-counter (Packard, Meriden, CT), and the data were presented as the mean counts per minute (CPM) minus the background (medium alone; ΔCPM) (Kitamura et al., 2007).

2.9. Quantification of cytokine

Cytokine concentrations in each culture supernatant were quantified with either BD™ Cytometric Bead Array kit (BD Bioscience, San Diego, CA, USA) (Cook et al., 2001) or FlowCytomix™ multiplex kit (Bender MedSystems GmBH, Vienna, Austria). In brief, as for CBA set-up, 50 μL samples or known concentrations of standard samples (0–5000 pg/ml) were added to capture beads conjugated with Ab for each cytokine followed by an addition of anti-cytokine Ab-phycoerythrin (PE) reagent (detection reagent). The mixture was then incubated for 2 h at room temperature in the dark, and washed to remove unbound detection reagent. As for FlowCytomix, 25 μL samples or known concentrations of standard samples (0–20 000 pg/ml) were added to capture beads conjugated with Ab for each cytokine followed by an addition of biotinylated anti-cytokine Abs and the mixture was incubated for 2 h at room temperature in the dark. After washing, the beads were incubated with streptavidin-PE for 2 h at room temperature in the dark, and washed to remove unbound detection reagent. Data acquisition was performed with FACS Calibur flow cytometer (BD Bioscience) and analyzed on a computer (CBA software 1.1; BD Bioscience or FlowCytomix Pro2.2 software). Amounts of IFN-γ, TNF-α and Interleukin (IL)-1α, -2, -4, -5, -6, -10, -17, and granulocyte macrophage colony-stimulating factor (GM-CSF) were quantified.

2.10. Statistical analysis

Data are presented as mean ± SD in clinical and histopathological scoring and as mean ± SEM in analyses of cell proliferation and cytokine production. Statistical analysis of EAU scoring was performed using the nonparametric Mann–Whitney U-test. Analyses of cell proliferation and cytokine production were performed using two-tailed Student's t-test. P values < 0.05 were considered statistically significant.

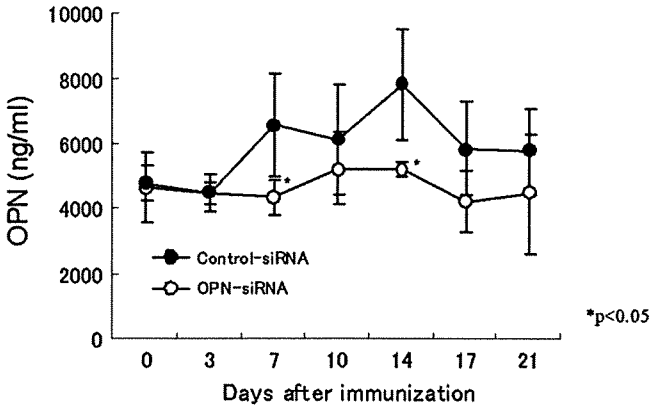

Fig. 1. Persistence of inhibition of plasma OPN level following *in vivo* siRNA treatment during EAU. EAU was induced in B6 mice. These mice were treated with OPN-siRNA (○) or control-siRNA (●) with hydrodynamic methods 24 h before and simultaneously with immunization. Blood was collected transcardially before immunization and on days 3, 7, 10, 14, 17 and 21 after immunization from each group of mice. All blood samples were collected under EDTA, centrifuged to remove cells and debris, and stored at −80 °C until used. Plasma levels of OPN were measured by sandwich ELISA. The results are presented as mean ± standard deviation. Statistical significance was determined using two-tailed Student's t-test (**, $P < 0.01$, *, $P < 0.05$). Data are representative of two separate experiments with the same result.

3. Results

3.1. OPN-siRNA treatment inhibited the increase of OPN plasma level during EAU

We demonstrated that the plasma concentration of OPN elevated from the basal level (4–5 μg/ml) over time after $IRBP_{1-20}$, peaked around 14 d, and then gradually waned (Kitamura et al., 2007), suggesting that plasma OPN concentration correlates well with disease development. First, we quantified the plasma OPN level to examine whether administration of OPN-siRNA could actually reduce the OPN level *in vivo*. To this end, we introduced siRNA twice at 24 h before and at the same time of $IRBP_{1-20}$ immunization. In the control-siRNA-treated group, OPN concentration in plasma again peaked around 2 wk, thus reproducing our previous results. On the other hand, in the OPN-siRNA-treated group, the OPN concentration in plasma was not elevated from the basal level during EAU. In comparison with that of the control group, plasma concentration of OPN upsurge was significantly

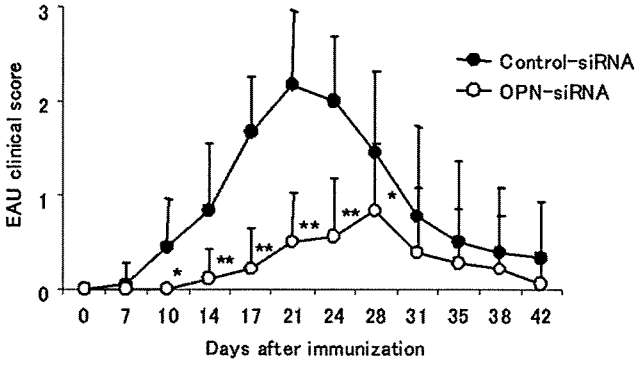

Fig. 2. Clinical score of EAU in mice treated with OPN-siRNA, 24 h before and simultaneously with the immunization. EAU was induced in B6 mice. These mice were treated with OPN-siRNA (○) or control-siRNA (●). Funduscopic examination was carried out every 3 or 4 days from day 7 after immunization. The results are presented as mean clinical score for all eyes of each group of mice (9 mice per group) ± standard deviation. Significance was determined using Mann–Whitney U-test (**, $P < 0.01$, *, $P < 0.05$).

suppressed following immunization in the OPN-siRNA-treated group at days 7 and 14 (Fig. 1).

3.2. OPN-siRNA reduced EAU scores

To investigate the potential of OPN-siRNA to prevent EAU, B6 mice were immunized with $hIRBP_{1-20}$ and treated twice with either OPN-siRNA or control-siRNA 24 h before and simultaneously with immunization. From day 7 after immunization, clinical assessment was performed every 3 or 4 days. As compared to the control group, the EAU clinical score was low in the OPN-siRNA-treated group during the entire period of observation (Fig. 2). In the OPN-siRNA-treated group, EAU reached a peak at day 28 after immunization. In contrast, control group mice peaked at day 21 (Fig. 2). The maximum clinical scores were significantly lower in the OPN-siRNA-treated group (average scores: 0.89 ± 0.68) than those in the control-siRNA-treated group (2.44 ± 0.78).

To further examine the effect of OPN-siRNA on EAU, histopathological examinations were performed. Eyes were removed from either OPN-siRNA- or control-siRNA-treated EAU mice 21 days after $hIRBP_{1-20}$ immunization. Representative histopathology of the eyes from mice treated with control-siRNA or OPN-siRNA is shown in Fig. 3A and B, respectively. In control mice, inflammatory cells were found in the retina, vitreous and choroid along with retinal folds and granulomatous lesions (Fig. 3A). Retinas collected from some mice treated with OPN-siRNA showed almost normal histology (Fig. 3B). The histological scores of retinal sections were significantly lower in OPN-siRNA-treated mice (average scores: 0.88 ± 0.69) than in control mice (1.5 ± 0.73; Fig. 3C).

3.3. OPN-siRNA treatment only partly reversed the disease

We next examined whether OPN-siRNA treatment could reverse an ongoing disease process. EAU was induced as usual by $hIRBP_{1-20}$

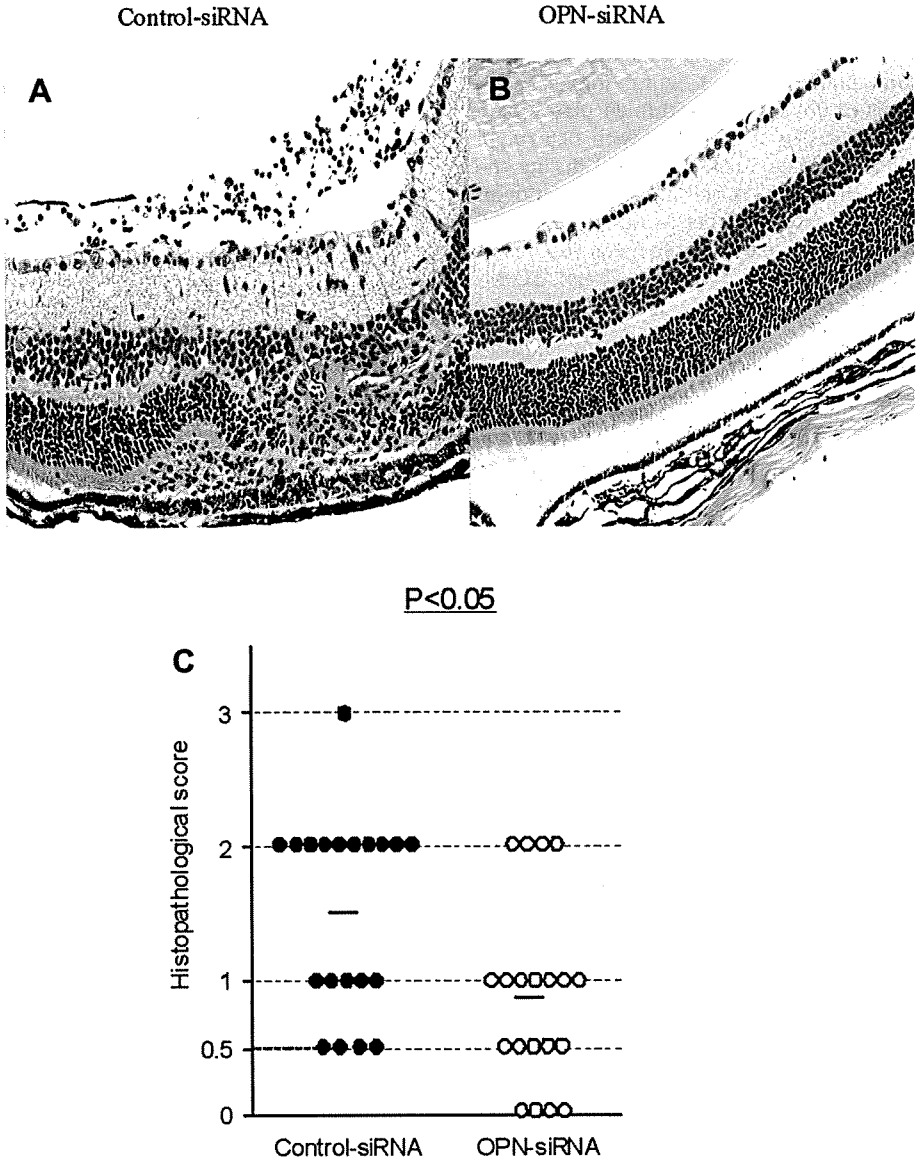

Fig. 3. Histopathology and histopathological score of EAU mice treated with OPN-siRNA. EAU was induced in B6 mice. Histopathology of mice treated with either control-siRNA (A) or OPN-siRNA (B). Note that inflammatory cells are present in the retina, vitreous, and choroid with retinal folds and granulomatous lesions in mice treated with control-siRNA (A) and the almost normal architecture of the retina in OPN-siRNA-treated mice (B). C. Mice were treated with OPN-siRNA (○) or control-siRNA (●). On day 21, the eyes were enucleated and scored by examining the histopathological sections of these eyes as shown in A and B. The results are presented as the histopathological score of each eye, and the mean EAU score of each group is indicated by a bar. Significance was determined by Mann–Whitney *U*-test ($P < 0.05$).

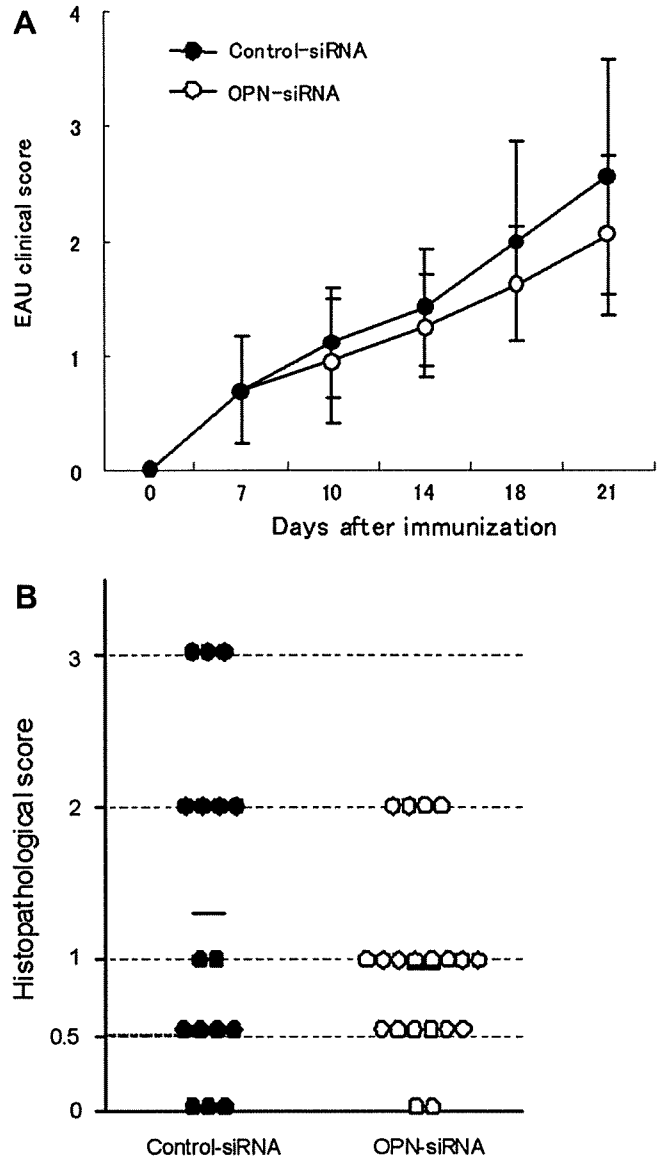

Fig. 4. Clinical and histopathological score of EAU in mice treated with OPN-siRNA with reversal regimen. A. EAU was induced by $hIRBP_{1-20}$ immunization at day 0. These mice were treated with two injections of either OPN-siRNA (○) or control-siRNA (●) on day 7 and day 8 after the immunization. Funduscopic examination was carried out every 3 or 4 days from day 7 after immunization. The results are presented as mean clinical score for all eyes of each group of mice (10 mice per group) ± standard deviation. Representative data of two separate experiments with similar results are presented. B. Histopathological score of EAU in mice treated with OPN-siRNA with reversal regimen. On day 21, the eyes from EAU mice were enucleated and scored of each eye. The mean EAU score of each group is indicated by a transverse bar.

immunization at day 0, and the mice were treated with two injections of either OPN- or control-siRNA at day 7 and day 8 when ocular symptoms first appeared overt after the immunization (reversal regimen). The clinical severity of EAU appeared to be slightly lower around day 21 but was not significantly reduced during the course of observation with the reversal regimen (Fig. 4A). The histopathological scores of retinal sections were not significantly lower in OPN-siRNA-treated mice (average scores: 0.95 ± 0.63) than in control mice (1.31 ± 1.11; Fig. 4B).

These results suggest that OPN-siRNA treatment more efficiently targets the priming rather than effector function of pathogenic T cells.

3.4. OPN-siRNA showed a slight influence on priming of hIRBP-specific T cells, but significantly inhibited Th1 and Th17 cytokine responses

To examine the mechanism underlying the suppressive effect of siRNA, we analyzed proliferative responses of lymphocytes from regional lymph nodes of hIRBP-immunized mice treated with OPN-siRNA or control-siRNA upon stimulation with hIRBP *in vitro*. As shown in Fig. 5A, lymphocytes from both groups mounted a considerable response. No significant differences were observed in the cell proliferation between OPN-siRNA-treated and control-siRNA-treated EAU mice, although the response in the OPN-siRNA group was slightly lower than that in the control group.

Next, we examined cytokine levels in the cultures of hIRBP peptide and lymphocytes collected from hIRBP-immunized mice treated with either OPN-siRNA or control-siRNA. We quantified IFN-γ and TNF-α concentrations in the culture supernatants. The levels of both IFN-γ and TNF-α were significantly reduced in the supernatants from cells of siRNA-treated mice compared to those of control-siRNA-treated mice at any concentrations of hIRBP analyzed (Fig. 5B). Furthermore, the production levels of IL-2, GM-CSF, and IL-17 were also significantly reduced in the supernatants from cells of OPN-siRNA-treated mice compared to those of control-siRNA-treated mice, whereas there no difference in the production of IL-1α, -4, 5, 6, and 10 between the two groups (Fig. 5C, and data not shown).

4. Discussion

In our previous study (Kitamura et al., 2007), we demonstrated that the plasma OPN levels were significantly elevated in EAU B6 mice by day 3 after immunization and peaked at day 14, which was concordant with the clinical course. Notably, OPN knockout (KO) mice displayed a considerably milder EAU and delayed disease onset compared with those of $OPN^{+/+}$ littermates (Hikita et al., 2006; Kitamura et al., 2007). In addition, EAU induced in B6 mice was ameliorated by administration of M5, an anti-OPN antibody. These findings demonstrated that OPN played a role in EAU development and might be an appropriate target for controlling ocular inflammation.

In the present study focusing on the blockade of OPN production, we used siRNA targeting the OPN coding sequence (OPN-siRNA). The OPN-siRNA was introduced into the animal with a hydrostatic pressure-mediated technique, hydrodynamic delivery (Liu et al., 1999). OPN is thought to function not only in soluble form (OPN-s) as a cytokine but also in intracellular form, OPN-i (Shinohara et al., 2006; Cantor and Shinohara, 2009). Although anti-OPN Ab can only be accessible to and block OPN-s, OPN-siRNA may block both forms by reducing the expression in both compartments.

First, we quantified the plasma level to evaluate the duration for the inhibition of OPN following *in vivo* siRNA treatment with the prevention regimen (day 1 and 0 of immunization) in EAU mice. OPN-siRNA treatment inhibited the increase of the plasma OPN level during the entire period of EAU to the basal level (Fig. 1). It was reported that OPN protein expression was significantly suppressed 5 days after *in vitro* siRNA treatment (Saito et al., 2007). In our study, OPN level remained significantly reduced at day 7 and day 14 in the OPN-siRNA-treated group (Fig. 1). This result suggested that OPN-siRNA treatment could have a longer period of efficacy than anticipated and thus may be applicable to chronic inflammatory diseases. When RNAi for OPN was induced with a prevention regimen, significant prevention of EAU was indeed manifested as had been shown with anti-OPN Ab (M5) treatment (Figs. 2 and 3). As to the clinical score, OPN-siRNA appeared to be more efficient than M5 (Kitamura et al., 2007).